75-pg column; GE Healthcare). Molecular weight standards (Gel Filtration Calibration kits LMW; GE Healthcare) were used to estimate the molecular weights of CTB, Pvs25H-A, and their fusion complex by calculating the partition coefficient (K_{av}) values for each protein standard and sample protein.

Immunization with CTB-Pvs25H-A fusion protein and analysis of induced antibodies. Eight-week-old female BALB/c mice were purchased from Japan SLC (Shizuoka, Japan). Mice (four or eight mice per group) were immunized via the s.c. or the i.n. route with 30 μg of Pvs25H-A, a mixture of CTB and Pvs25H-A (30 μg each) or 60 μg of CTB-Pvs25H-A fusion protein. Where indicated, incomplete Freund's adjuvant (IFA; Difco Laboratories, Detroit, MI) or 0.1 to 1.0 μg of CT (List Biological Laboratories, Campbell, CA) was used for s.c. or i.n. adjuvants, respectively. The mice were immunized three times, at weeks 0, 2, and 3.

Mice were anesthetized 1 week after the third immunization (week 4) by intraperitoneal injection of pentobarbital sodium salt (Nacalai Tesque, Inc.) and were sacrificed by exsanguination to collect serum. For specific serum antibody analysis, ELISA plates (Sumilon; Sumitomo Bakelite Co.) were coated with Pvs25H-A (5 μg/ml) in bicarbonate buffer by incubating the plate at 4°C overnight. The plate was washed twice with PBS-T and once with PBS. The plate was blocked with 1% bovine serum albumin (BSA) in PBS for 2 h at 37°C. Twofold serial dilutions of the antisera starting with 50-fold dilution with 0.5% BSA in PBS were applied to the wells in duplicate, which were then incubated for 2 h at 37°C. The plate was then incubated with anti-mouse IgG conjugated to alkaline phosphatase (1/4,000; Sigma-Aldrich) for 2 h at 37°C. *p*-Nitrophenylphosphate (Bio-Rad) was added to the plate for color development, and the absorbance at OD_{415} was measured after 20 min of incubation at 37°C, using a microplate reader (Bio-Rad). The antibody titer was defined as the serum dilution that gave an OD_{415} value equal to 0.1 or as the serum dilution where a one magnitude higher dilution gave an OD_{415} value of <0.1.

All animal experimental protocols were approved by the Institutional Animal Care and Use Committee of the University of the Ryukyus, and the experiments were conducted according to the Ethical Guidelines for Animal Experiments of the University of the Ryukyus.

Mosquito membrane feeding assay. Heparinized syringes were used for peripheral blood collection, with written informed consent, from *P. vivax* patients who came to a malaria clinic in the Mae Sod district in the Tak province of northwestern Thailand. Single species infection with *P. vivax* was confirmed by Giemsa stain of thick and thin blood smears. The levels of parasitemias and the gametocytemias were 0.22 and 0.02%, respectively, for the volunteer *P. vivax* patient 1, and 0.23 and 0.01%, respectively, for the volunteer *P. vivax* patient 2. Collected blood was aliquoted into tubes (300 μl/tube), and the plasma was removed after brief centrifugation. Pooled mouse antisera were mixed with an equal volume of heat-inactivated normal human AB serum prepared from malaria-naive donors. The test antiserum sample was mixed and incubated with *P. vivax*-infected blood cells (1:1 [vol/vol] ratio) for 15 min at room temperature. The mixture was then applied to a membrane feeding apparatus kept at 37°C to allow starved *Anopheles dirus* A mosquitoes (Bangkok colony, Armed Forces Research Institute of Medical Sciences) to feed on the blood meals for 30 min. Fully engorged mosquitoes were separated from unfed mosquitoes, maintained for a week in an insectary kept at 26°C, and provided with 10% sucrose water. For each blood sample-serum mixture, 20 mosquitoes were dissected, and the number of oocysts in the midgut was counted under a microscope after 0.5% mercurochrome staining.

All human subject research conducted in the present study was reviewed and approved by the Ethics Committee of the Thai Ministry of Public Health and the Institutional Review Board of the Walter Reed Army Institute of Research.

Detection of native Pvs25 in antisera from immunized mice. Peripheral blood from *P. vivax*-infected patients was collected as described above. The gametocytemic patient blood was used to grow zygotes and ookinetes *in vitro*, as described previously (23). They were spotted onto slides and fixed with acetone as described previously (1–3). The slides were blocked with 5% nonfat milk in PBS and incubated with mouse antisera derived from immunization with CTB-Pvs25H-A fusion protein emulsified with IFA or with the fusion protein supplemented with CT (1 μg), after dilution of the antisera 100-fold with 5% nonfat milk in PBS. The samples were washed with ice-cold PBS and incubated with Alexa 488-conjugated anti-mouse antibody (Invitrogen, Carlsbad, CA). After a wash with ice-cold PBS, the slides were viewed by confocal scanning laser microscopy (LSM5 Pascal; Carl Zeiss MicroImaging, Thornwood, NY).

Statistical analysis. The Wilcoxon-Mann-Whitney test was used to compare antibody titers or the number of oocysts per mosquito between the nonimmune and an indicated immunization group or between indicated two immunization groups. The Kruskal-Wallis test was used to compare antibody titers or the number of oocysts per mosquito among three groups (i.e., S, M, and L). The chi-square test was used to analyze the difference in the proportion of parasite-free mosquitoes out of the total number of mosquitoes examined between the nonimmune and an indicated immunization group or between indicated two immunization groups. All statistical analysis were conducted by using JMP software version 8.0 (SAS Institute, Inc., Cary, NC).

RESULTS

Expression and purification of recombinant Pvs25H-A isoform from *P. pastoris*. Ookinete surface proteins (OSPs) contain several intramolecular disulfide bonds, e.g., the 11 disulfide bonds in Pvs25, which are important for overall structural integrity and native antigenicity. For this reason, *E. coli* expression systems are unsuitable, and therefore yeast *Saccharomyces cerevisiae* expression systems are used (12, 15, 19, 22). We explored other, more efficient recombinant protein expression systems for Pvs25 and found a higher production efficiency in the yeast *P. pastoris*. We constructed a plasmid for secretory expression of Pvs25 as a C-terminal hexahistidine-tagged protein (Pvs25H) (Fig. 1a). The culture supernatant of recombinant *P. pastoris* was found to contain several protein species that were not present in the culture supernatant of vector-transformed clones (Fig. 1b), and these protein bands specifically reacted with anti-Pvs25 antiserum, as well as with an anti-hexahistidine tag monoclonal antibody (data not shown). Secreted Pvs25H was affinity purified on a nickel Sepharose column and further separated into large (fractions 16 to 19) and small (fractions 21 to 23) protein species by size exclusion chromatography (Fig. 1c and d). At least five protein bands were identified on SDS-PAGE (Fig. 1b) and their corresponding peaks by size exclusion chromatography (fractions 16, 17, 18-19, 21-22, and 22-23 in Fig. 1c and d). The apparent molecular masses of these protein species based on gel mobility on SDS-PAGE were estimated to be 63.2, 47.3, 33.2, 16.1, and 28.3 kDa, respectively. The calculated molecular mass of Pvs25H (based on its deduced amino acid sequence) is 20.2 kDa, to which the fraction 21 and 22 protein species corresponded most closely. We therefore concluded that this was monomeric Pvs25H. Furthermore, the apparent molecular masses of protein species found in fractions 18 and 19, 17, and 16 corresponded very well to multiples of the molecular mass of the apparent monomer, so we concluded that they represented the dimer, trimer and tetramer of Pvs25H, respectively. The protein species that appeared in fractions 22 and 23 exhibited markedly different gel mobility (28.3 kDa) from that of the monomeric protein (16.1 kDa) (Fig. 1d), although these two showed extensively overlapping chromatographic peaks on size exclusion chromatography (Fig. 1c). We concluded that the protein species in fractions 22 and 23 was a monomeric protein with a distinct hydrophobic character, and thus decided to further separate these two monomers based on hydrophobicity profile by HIC. HIC clearly separated the two monomeric isoforms (Fig. 1f), and we named the less hydrophobic isoform and the more hydrophobic isoform the A and B monomeric isoforms, respectively (19). The observed lower gel mobility for the A isoform than the B isoform on SDS-PAGE under nonreducing conditions (Fig. 1d) was consistent with the results of HIC: the more hydrophilic the molecule, the fewer SDS molecules bind, and the protein becomes less negatively charged, resulting in reduced gel mobility on SDS-PAGE.

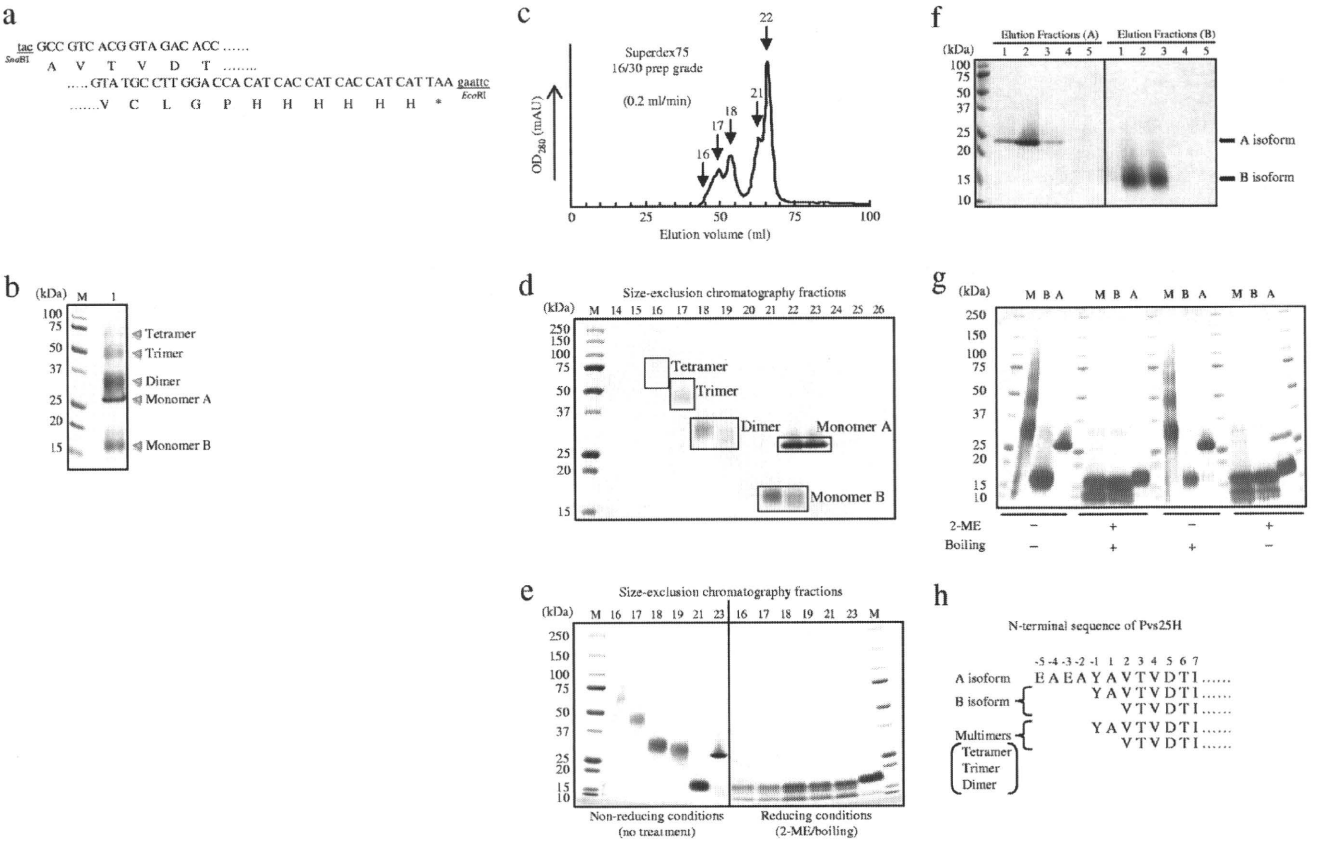

FIG. 1. Construction and expression analysis of Pvs25H in *Pichia pastoris*. (a) The 5′- and 3′-coding regions of the *Pvs25* gene sequence with its predicted amino acid sequence (Ala_{23} to Leu_{195}). The *Pvs25* gene fused to a hexahistidine tag at its C terminus was inserted into the SnaBI and EcoRI sites of pPIC9K, and the gene was integrated into the chromosomal DNA of *P. pastoris* strain GS115 by homologous recombination. (b) After selection of a high-producer clone that secreted the recombinant protein, nickel-affinity chromatography-purified Pvs25H was analyzed by SDS-PAGE (lane 1). M, molecular marker. (c) The affinity-purified Pvs25H was fractionated by size exclusion chromatography from which at least five chromatographic peaks were observed. (d) Size exclusion chromatography fractions 14–26 were subjected to SDS-PAGE (15% acrylamide). Based on the apparent molecular mass of each protein band, the fractions 16, 17, 18-19, 21-22, and 22-23 were defined as the tetramer, trimer, dimer, monomer B, and monomer A, respectively. (e) Selected chromatography peaks were subjected to 5 to 20% acrylamide gradient SDS-PAGE under nonreducing or reducing (10% 2-ME and boiling) conditions. (f) Hydrophobic interaction chromatography of the Pvs25H-A and Pvs25H-B monomeric isoforms. Elution fractions (A) are eluates of 2 M NH_4SO_4 (Pvs25H-A) and elution fractions (B) are eluates of PBS (Pvs25H-B). (g) Each isoform (M, a mixture of dimer, trimer and tetramer; B, B isoform; A, A isoform) was subjected to 15% acrylamide SDS-PAGE under various conditions, as indicated. (h) The N-terminal protein sequence of each isoform. Positively numbered amino acid residues (Ala_1 and the following) are residues of the Pvs25 protein; negatively numbered amino acids are derivatives of the pPIC9K α-factor secretion signal. The A monomer revealed a single, unique sequence, but the B monomer and the multimers showed a mixture of different N termini.

Molecular characterization of Pvs25H isoforms. The A isoform appeared as a single sharp band, but the other isoforms, including the multimers and the B monomer, appeared as diffuse bands on SDS-PAGE (Fig. 1b and d to g), indicating that the A isoform is constrained to a more uniform molecular configuration than the other isoforms. In addition, all of the isoforms, except the A isoform, generated at least three identical protein bands when samples were heat treated in the presence of SDS and β-mercaptoethanol (2-ME) prior to SDS-PAGE. The A isoform appeared as a single protein band with a slightly higher molecular mass than that for the largest protein band among the three bands observed for the other isoforms (Fig. 1e).

To characterize the molecular configuration of each isoform furthermore, mixtures of the multimers, including dimers, trimers, and tetramers and the A and B monomers, were subjected to SDS-PAGE after various treatments, as indicated in Fig. 1g. The gel mobility of all of the isoforms did not show any noticeable changes after boiling (100°C, 2 min), but 2-ME treatment (10% [vol/vol]) resulted in a banding pattern very similar to the pattern observed for complete denaturation (2-ME and boiling), except that the A isoform seemed to be slightly more resistant to the reducing agent than the other isoforms. This became particularly notable when lower concentrations of the reducing agent were used (data not shown). These results suggest that the multimers comprised B monomers self-cross-linked by intermolecular disulfide bonds and that the A isoform has a higher molecular rigidity than the other isoforms. Because all of the isoforms exhibited a strong resistance to the boiling and SDS, but not to the 2-ME and SDS treatment, it is plausible that the physical integrity of the protein is critically, if not completely, maintained by disulfide bonds.

Next, to evaluate the status of the covalent disulfide bonds in

the Pvs25H protein, Ellman's test was conducted for each isoform. No isoform reacted with the Ellman's reagent, suggesting either that no reduced sulfhydryls were present or that the molecules were inaccessible to the reagent. However, treatment with TCEP immobilized on agarose prior to the Ellman's test resulted in the detection of 4 to 6 molecules of reduced sulfhydryls per molecule of B monomer or multimeric isoforms, but fewer than 0.3 molecules of reduced sulfhydryls were detected per molecule of A monomer. These results indicated that the B and multimeric isoforms have disulfide bonds that are more accessible to surface-immobilized TCEP than those of the A isoform, indicating that the A isoform has more deeply buried disulfide bonds than the other isoforms. It is indicative of the higher molecular flexibility of the B isoform and the multimers than of the A isoform. Interestingly, however, denaturation of proteins with 2% SDS or 6 M guanidine hydrochloride, or TCEP agarose treatment in the presence of these denaturants prior to the Ellman's test, did not further increase the level of free sulfhydryls. These results strongly support the notion that all of the isoforms are tightly packed molecules and that their rigidity is maintained by intramolecular disulfide bonds and other noncovalent interactions.

Finally, the N-terminal protein sequences determined by the Edman degradation method for each isoform supported the results of SDS-PAGE, in that the multimers and the B isoform contain a mixture of polypeptide species with multiple N termini; however, the A isoform comprises a single polypeptide with a longer, unique N terminus (Fig. 1h). These results suggested that the multimers and the B isoform contain the same set of polypeptide species, with multiple primary structures and presumably various folding configurations. By using different combinations of structurally heterologous polypeptides, different isoforms might be generated.

Taken together, we concluded that the A isoform, which has a more uniform protein configuration, is less hydrophobic and has higher molecular rigidity than the B isoform, and perhaps it most closely resembles the native Pvs25 protein at the structural level. The proportions of each isoform expression were estimated to be 42% (A isoform), 27% (B isoform), 16% (dimer), 10% (trimer), and 5% (tetramer). Thus, the A isoform was produced most abundantly among all of the isoforms. The final protein yields of the total Pvs25H and the A isoform using our expression and purification method were 30 to 50 mg and 12 to 20 mg/liter of culture medium, respectively. We confirmed that the purified Pvs25H-A contained endotoxin at levels less than 0.05 EU/μg of protein. Based on these observations, we decided to use the A isoform (Pvs25H-A) as a TBV antigen to be linked to CTB.

Chemical conjugation of Pvs25H-A to CTB and its molecular evaluation. Recombinant CTB was expressed by *P. pastoris* strain GS115 and purified as previously reported (11). Pvs25H-A was chemically conjugated to CTB by using the heterobifunctional cross-linker SPDP (Fig. 2). Because CTB contains two cysteine residues per monomeric subunit, which, in the native form, are involved in an intramolecular disulfide bond, the existence of reduced sulfhydryls in our recombinant CTB was determined by using Ellman's reagent, and none was detected (data not shown).

Various conjugation schemes were evaluated for efficiency of linking Pvs25H-A to CTB via SPDP (Fig. 2a and b). Consistent with the results of Ellman's test for Pvs25H-A and CTB, SPDP modification of only one protein failed to generate the CTB-Pvs25H-A fusion complex (Fig. 2b). Thus, at least one partner protein had to be treated with the reducing agent to expose free sulfhydryls and make it reactive toward the pyridyldithiol groups added to the partner protein. Because intact disulfide bonds might be important for the overall structural integrity and native antigenicity of Pvs25 (12, 15, 19, 22), we avoided treating it with reducing agents. Therefore, the CTB or SPDP-modified CTB (CTB^{SPDP}) was treated instead with DTT (designated as CTB^{DTT} or $CTB^{SPDP/DTT}$ in Fig. 2a). Although both CTB^{DTT} and $CTB^{SPDP/DTT}$, when reacted with SPDP-modified Pvs25H-A ($Pvs25H\text{-}A^{SPDP}$), generated substantial levels of fusion complex with retained affinity for GM1-ganglioside, sequential treatment of CTB with SPDP and then with DTT resulted in an even higher specific reactivity toward Pvs25 antiserum (Fig. 2b).

Second, to evaluate the homogeneity of the fusion complex and the stoichiometry of each component within the complex, proteins before and after the conjugation process were analyzed by size exclusion chromatography (Fig. 2c). The two chromatographic peaks for Pvs25H-A and CTB in a mixed sample disappeared, and a new single peak emerged with an apparent molecular mass of 97.2 kDa. Because the molecular masses of Pvs25H-A and CTB are 29.8 and 53.4 kDa, respectively, based on the K_{av} values of chromatography standard proteins, the average stoichiometric ratio for CTB and Pvs25H-A was calculated to be 1:1.5, indicating that one CTB pentamer molecule carries one to two molecules of Pvs25H-A on its surface. Alternatively, if it is assumed that the fusion complex is highly homogeneous and its stoichiometric ratio is 1:1, the 14-kDa discrepancy between the observed and calculated fusion complex mass may be explained by irregularities in the molecular shape, resulting in a higher apparent molecular mass.

Taking all of the results together, we decided to use the $Pvs25H\text{-}A^{SPDP}$ + $CTB^{SPDP/DTT}$ conjugation method (Fig. 2d) to generate the fusion complex for all immunization experiments.

Immunogenicity in mice of Pvs25H-A and its fusion protein with CTB when administered by the s.c. or the i.n. route. BALB/c mice were immunized with Pvs25H-A (designated as "S" in Fig. 3 and 4), a mixture of Pvs25H-A and CTB (designated as "M" in Fig. 3 and 4), or CTB-Pvs25H-A fusion protein (designated as "L" in Fig. 3 and 4), by the s.c. or the i.n. route, with or without the indicated adjuvants, at weeks 0, 2, and 3. Antisera were collected at week 4, and the Pvs25H-A-specific IgG titers were determined (Fig. 3a). We demonstrated that: (i) s.c. immunization tended to induce a higher response than i.n. immunization in both the absence and the presence of adjuvants; (ii) the fusion protein (L) consistently induced a higher response than antigen alone (S) or the mixture of proteins (M), regardless of adjuvant supplementation; (iii) supplementation with adjuvants was required for substantial augmentation of the IgG response for both immunization routes; (iv) IFA significantly augmented the response elicited by unfused or CTB-mixed antigen, but CT only marginally affected the response elicited by these antigens; and (v) CT did not exhibit a dose-dependent augmentation effect on the IgG response in the dose range used in the present study (0.1 to 1.0

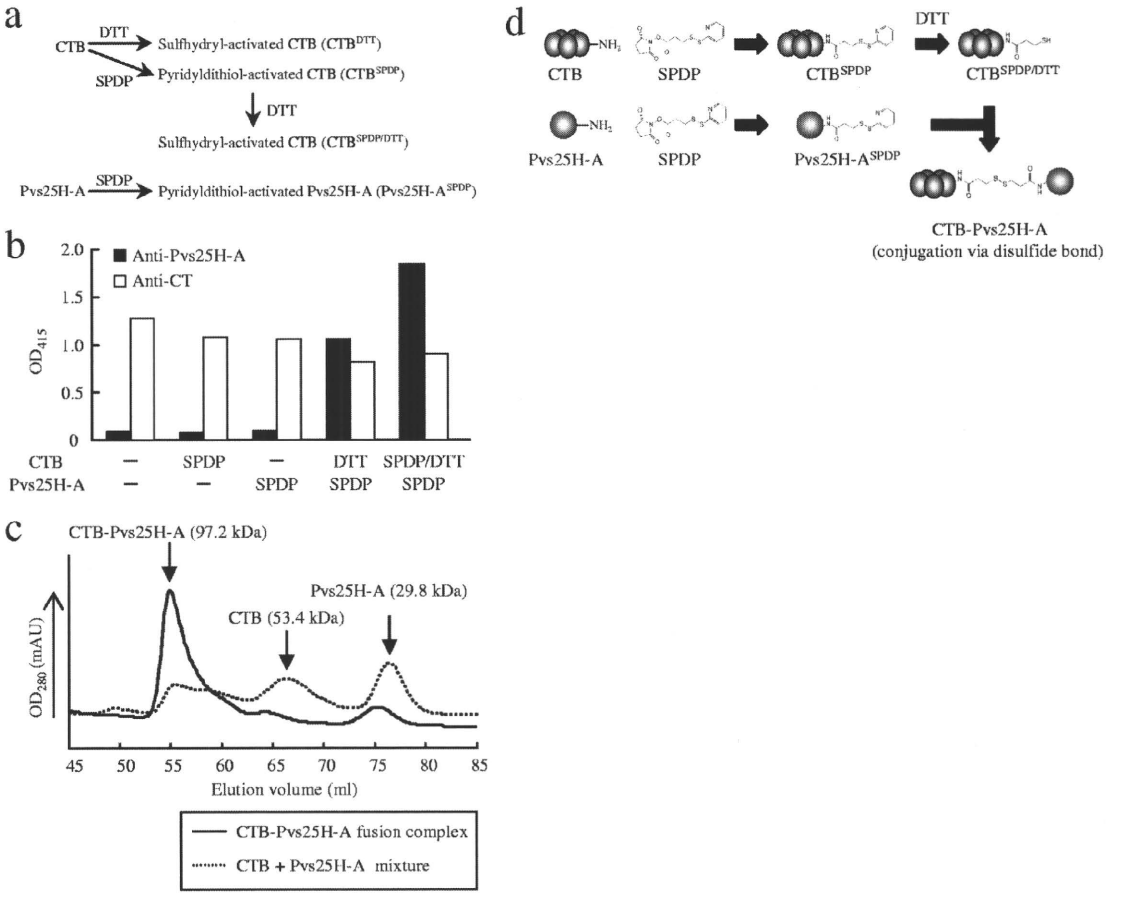

FIG. 2. Chemical conjugation of Pvs25H-A to cholera toxin B subunit (CTB). Various conjugation methods were evaluated for the generation of the CTB-Pvs25H-A fusion complex. The heterobifunctional cross-linker *N*-succinimidyl 3-(2-pyridyldithio) propionate (SPDP) was used to link Pvs25H-A to CTB via the primary amines. (a) Either CTB or SPDP-modified CTB (CTB^{SPDP}) was first treated with DTT to expose free sulfhydryls (designated as CTB^{DTT} and $CTB^{SPDP/DTT}$, respectively), and then SPDP-modified Pvs25H-A ($Pvs25H\text{-}A^{SPDP}$) was separately mixed with each of them to generate the fusion complex. (b) The CTB-Pvs25H-A fusion complex was analyzed by GM1-ELISA using anti-cholera toxin (CT) (□) or anti-Pvs25H-A (■) antiserum. (c) The CTB-Pvs25H-A fusion protein (solid line) or a mixture of CTB and Pvs25H-A (dotted line) was subjected to size exclusion chromatography. For the fusion protein, the peaks for CTB and Pvs25H-A disappeared, and a new peak emerged, indicating generation of the fusion complex. (d) The conjugation scheme chosen for production of the CTB-Pvs25H-A fusion complex. See Materials and Methods for the detailed conjugation method.

μg). Finally, we confirmed that the antisera specifically recognized the *P. vivax* ookinete surface by immunofluorescence (Fig. 3b).

Transmission-blocking effect of the induced mouse antisera against field strains of *P. vivax* parasites. The TBV efficacy of the induced mouse antisera against *P. vivax* parasites in infected blood samples from patients was evaluated by the membrane feeding assay. The same experiments were performed twice, using blood samples from two volunteer donors (Fig. 4). The average number of oocysts observed per mosquito fed on patient blood mixed with antisera induced by s.c. immunization of mice with Pvs25H-A/IFA was reduced by >99.9% compared to the naive control serum (N). Omission of the adjuvant significantly abated the effect down to 20 to 60% reduction; however, conjugating the antigen to CTB resulted in a dramatic restoration of the vaccine efficacy back to >90%. A similar tendency, albeit with significantly lower efficacy, was observed for i.n. immunization, in that antisera induced by i.n. immunization with the fusion protein decreased the oocyst number by 70 to 90%, whereas unfused antigen conferred only a 0 to 6% blocking effect. As expected, CT supplementation augmented the effect for i.n.-administered antigens, in that both unfused and CTB-fused antigens conferred a blocking effect of >90%. Interestingly, however, addition of CTB to the mixture of antigen and CT significantly abated the vaccine efficacy down to 40 to 50%. The reason for this is unknown, and it could not have been predicted from the antibody titers (Fig. 3a). Taken together, we concluded that chemical coupling of Pvs25 to CTB is a potentially promising strategy to enhance the transmission-blocking efficacy in i.n. and s.c immunization regimes.

DISCUSSION

Pvs25 is one of the top-priority *P. vivax* TBV candidates, and the production of stable and functional forms of the antigen in the most appropriate formulation is crucial (4; MVTR). In the present study, we investigated the methylotrophic yeast *P. pas-*

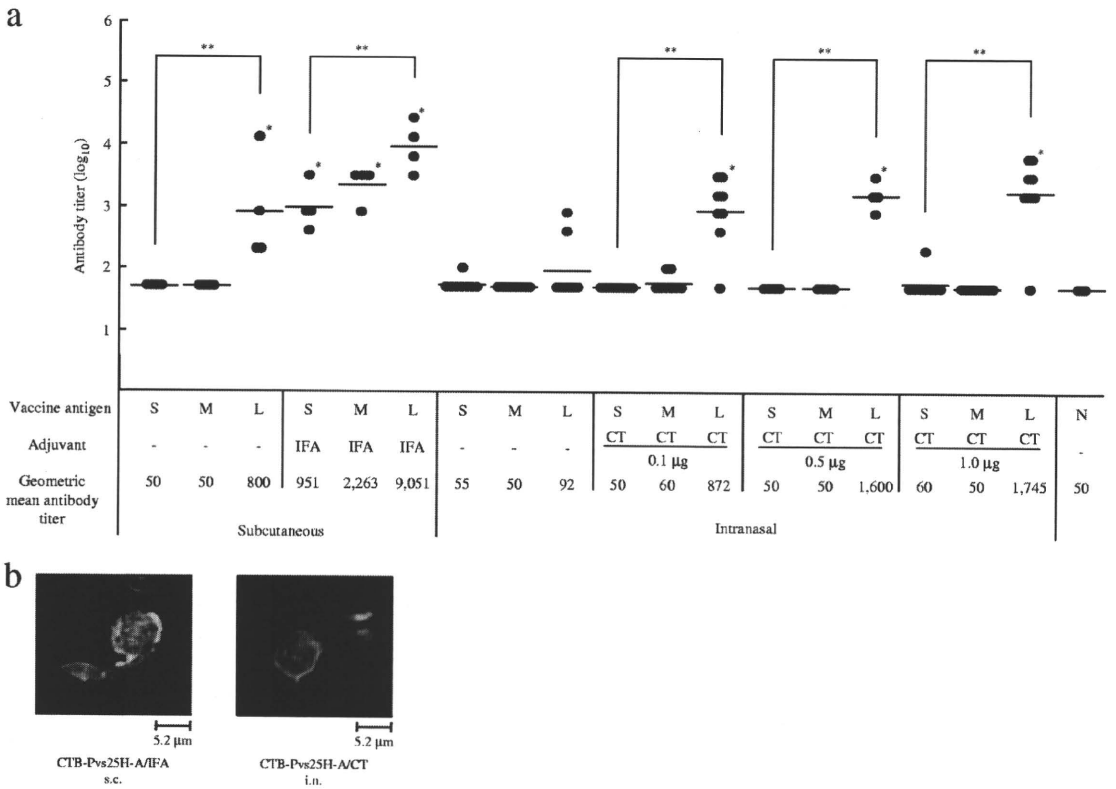

FIG. 3. Immunogenicity of the CTB-Pvs25H-A fusion protein for induction of a Pvs25-specific serum IgG response. (a) Female BALB/c mice (four or eight mice per group) were immunized with Pvs25H-A alone (30 μg) (S), a mixture of cholera toxin B subunit (CTB; 30 μg) and Pvs25H-A (30 μg) (M), or the CTB-Pvs25H-A fusion protein (60 μg), by the subcutaneous (s.c.) or the intranasal (i.n.) route (L), three times, at weeks 0, 2, and 3. Serum samples were collected a week after the third immunization and were evaluated for Pvs25-specific IgG titers. All mice received the same amount of Pvs25H-A antigen, i.e., 30 μg per injection. IFA and CT at various doses (0.1 to 1.0 μg) were used as s.c. and i.n. vaccine adjuvants, respectively. Nonimmune serum (N) was used as a negative control. Antibody titers were defined as the serum dilution that gave an OD_{415} of 0.1 or the serum dilution for which a one-point-higher dilution (2-fold) gave an OD_{415} of <0.1. *, Significantly different from nonimmune serum as determined by the Wilcoxon-Mann-Whitney test ($P < 0.05$); **, significantly different among the three groups (S, M, and L) as determined by the Kruskal-Wallis test ($P < 0.001$). (b) Ookinete-specific reactivity of induced antisera analyzed by immunofluorescence. The antisera derived from s.c. immunization with the CTB-Pvs25H-A fusion protein emulsified with IFA (CTB-Pvs25H-A/IFA), or the fusion protein administered i.n. with CT (1 μg) (CTB-Pvs25H-A/CT) specifically recognized native Pvs25 protein expressed on the surface of *Plasmodium vivax* ookinetes. Scale bar, 5.2 μm.

toris as a production host for Pvs25. The yield of Pvs25H was comparable to that reported previously for its expression in *S. cerevisiae* (19). When expressed in *S. cerevisiae*, this protein was also produced as a mixture of various isoforms (19). Although we observed a similar protein expression pattern, i.e., multimers and the A and B monomers, higher proportions of the molecularly homogeneous A isoform than the heterogeneous B and multimeric isoforms were produced when Pvs25H was expressed in *P. pastoris* and not in *S. cerevisiae*. This might present an advantage of using *P. pastoris* expression system for Pvs25 vaccine production rather than *S. cerevisiae* system. The *P. pastoris*-derived A isoform could be as conveniently and efficiently purified from the culture supernatant as reported for *S. cerevisiae*-derived A isoform, by a combination of affinity, size exclusion, and hydrophobic interaction chromatographies.

The next critical step in vaccine generation is the optimization of vaccine antigen formulations; a search for the optimal antigen formulation is often considered to be as important as choosing the best antigen among many vaccine candidate antigens. Pvs25H antigen adsorbed onto Alhydrogel (Brentag Biosector, Frederilssund, Denmark) has recently been shown to induce antibody effectively in human volunteers in a phase 1 clinical trial, and the antigen was found to be efficacious, as evidenced by significant transmission-blocking activity observed in the membrane feeding assay (17). That study confirmed that Pvs25 is a very promising TBV candidate; however, it is highly desirable to induce higher levels of transmission-blocking immunity for practical vaccine development (17). Another phase 1 clinical trial using Montanide ISA 51, a water-in-oil emulsion, has recently been completed; however, due to an unexpected frequent local reactogenicity, the vaccine efficacy has not been verified (29). Therefore, there seems to be an increasing demand for the development of a new immune-enhancing vaccine platform technology for malaria OSPs, because they are low-molecular-weight proteins that are by themselves not sufficiently immunogenic.

There have been several reports showing examples of chemical conjugation of *Plasmodium falciparum* OSPs with potential antigen carrier molecules such as the outer membrane protein of *Neisseria meningitidis* (30), exoprotein A of *Pseudomonas*

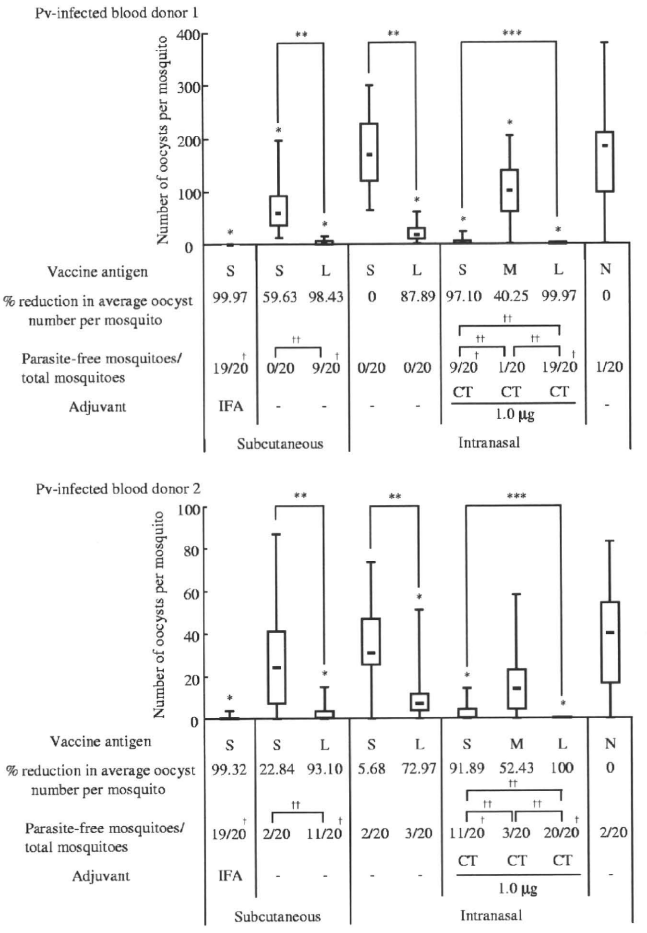

FIG. 4. Transmission-blocking vaccine (TBV) effects of the induced mouse antisera on *Plasmodium vivax* oocyst development in the *Anopheles dirus* A mosquito midgut. TBV effects on oocyst numbers induced by antisera (1/2 dilution) obtained from mice immunized with each antigen formulation (S, M, and L) as described in Fig. 3. N, nonimmune serum. Either IFA or CT was used as an adjuvant, as indicated. The data are expressed as the median values of oocyst number found per mosquito (bar within the box) with the 25 and 75% quartiles (the box) and ranges (whiskers above and below the box). The percent reduction was calculated as the reduction in the average oocyst number for each immunization group compared to the average oocyst number for the unimmunized control group (N). The number of parasite-free mosquitoes per total number of mosquitoes examined (20 mosquitoes) is provided. The analysis was performed twice, using different blood samples, as indicated in the upper panel (*P. vivax* [Pv]-infected blood donor 1) and the lower panel (Pv-infected blood donor 2). M groups without adjuvant supplementation, M and L groups with IFA supplementation, and all groups with 0.1- and 0.5-μg CT supplementation were excluded from membrane feeding analysis. *, $P < 0.001$ versus the nonimmune (N) group as determined by the Wilcoxon-Mann-Whitney test; **, $P < 0.001$ between the S and L groups as determined by the Wilcoxon-Mann-Whitney test; ***, $P < 0.001$ among the three groups (S, M, and L) as determined by the Kruskal-Wallis test; †, $P < 0.005$ versus the nonimmune (N) group as determined by the chi-square test; ††, $P < 0.005$ between the indicated two groups as determined by the chi-square test.

aeruginosa (16), ovalbumin (16), and a *P. falciparum* OSP itself by chemical crosslinking (16). All of these were demonstrated to increase TBV efficacy, but no attempts have yet been made to enhance the immunogenicity of *P. vivax* OSPs by coupling them to other proteins. In the present study we evaluated CTB as a potential carrier for Pvs25. First, to extend our previous study where CT was used as adjuvant (1–3), we tested our hypothesis that the mucosal immunogenicity of Pvs25 would increase when the protein was coupled to the nontoxic CTB subunit, even in the absence of CT supplementation. Second, to explore CTB's less-characterized immune potentiating properties for s.c.-delivered antigens, we immunized mice with the CTB-Pvs25H-A fusion protein by an s.c. route, in the presence or absence of IFA. Our principal finding was that the coupling of the antigen to CTB profoundly enhanced its immunogenicity in i.n. as well as in s.c. immunization regimes, without supplementation with extraneous adjuvants. However, the membrane feeding assay revealed that there was still much room for improvement (Fig. 4). For instance, although i.n. administration of the fusion protein alone conferred a relatively high transmission-blocking immunity (88 and 73% decreases in oocyst number for blood samples from donors 1 and 2, respectively) compared to unfused antigen alone or the unimmunized control group, only a few mosquitoes (0/20 to 3/20) were free of parasites. Supplementation of CT to the fusion protein increased the efficacy close to complete blockade (>99.9%), significantly increasing the number of mosquitoes free of parasites (19/20 to 20/20). Because supplementation of CT to unfused antigen resulted in an intermediate level of protection (97% [9/20] and 92% [11/20] decrease in oocyst number for blood samples from donors 1 and 2, respectively), we concluded that both the CT supplementation and the CTB-coupling strategies contributed to the increased vaccine efficacy, although the former was more efficient than the latter. A similar tendency was observed for the s.c. immunization regime: s.c. administration of the fusion protein alone conferred a more than 90% decrease in oocyst number, in which approximately half of the mosquitoes were free of parasites (9/20 to 11/20); however, the use of IFA with unfused antigen contributed more than the fusion method. We observed that the efficacy of the fusion protein administered alone by the s.c. route was almost equal to that attained by the unfused antigen administered i.n. with CT supplementation, in terms of the average numbers of oocyst per mosquito (>90%) as well as the number of mosquitoes free of parasites (9/20 to 11/20). Similarly, the vaccine efficacy for unfused antigen administered s.c. with IFA was almost equal to the level attained by the fusion protein administered i.n. with CT in terms of the average number of oocysts per mosquito (>99%) as well as the number of mosquitoes free of parasites (19/20 to 20/20). Although we did not assess the vaccine efficacy of the fusion protein emulsified in an oil adjuvant such as IFA, IFA was very effective in that almost complete blockade was observed for unfused antigen. It is likely that a combination of oil adjuvant and the CTB-coupling strategy would further enhance the efficacy. Taken together, we conclude that (i) s.c. immunization is more efficacious than i.n. immunization, inducing "one-level-higher" immunity than i.n. immunization, and (ii) a CTB-coupling strategy is substantially effective in enhancing transmission-blocking immunity, but supplementation with extraneous adjuvants is expected to induce an even higher immunity (Fig. 5).

The clinical use of CT, particularly as a nasal adjuvant, is hampered by its toxicity (26). Furthermore, the nontoxic CTB has yet to be proven a safe nasal vaccine delivery molecule.

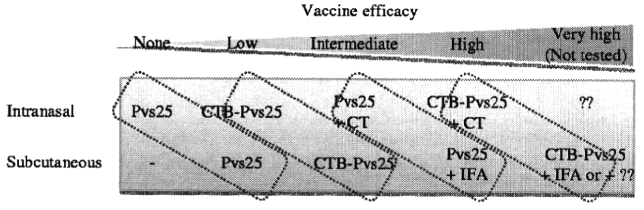

FIG. 5. Schematic summary of the observed or expected (but not tested) transmission-blocking vaccine (TBV) efficacy induced by each immunization regime. s.c. immunization tended to induce "one-level-higher" immunity than i.n. immunization in our experimental model. Identical or similar vaccine formulations are encircled by a dotted line. CTB, cholera toxin B subunit; CT, cholera toxin; IFA, incomplete Freund's adjuvant.

Therefore, an alternative approach for using CTB as a vaccine antigen carrier is highly desirable. Although there have been numerous reports demonstrating enhanced mucosal immunogenicity of various antigens by coupling to CTB (13), very few systematic studies have been conducted to assess CTB's antigen carrier capacity for s.c.-delivered antigens. Our present study clearly demonstrated the potential of CTB in s.c. vaccine platform design. Furthermore, it is notable that, unlike antigens emulsified with oil adjuvant such as IFA or antigens administered with an aluminum hydroxide adjuvant, the protein-only CTB-coupled antigens are likely to be much less reactogenic. It is believed that recent innovations in effective but much less locally reactogenic and safer oil adjuvants such as MF59 (Chiron Corp., Emeryville, CA) (20, 21), the Montanide ISA series (Seppic, Inc., Fairfield, NJ) (20, 29), and the GlaxoSmithKline adjuvant systems (GlaxoSmithKline, Brentford, United Kingdom) (8, 27), will expedite malaria vaccine development. It is also possible that protein delivery molecules will ultimately be combined with effective oil or other adjuvants, including aluminum hydroxide. This is supported by our recent unpublished study in which a recombinant malaria antigen administered with an alum adjuvant only marginally enhanced its immunogenicity, whereas the same antigen loaded onto carrier molecules became highly immunogenic when applied together with the alum.

In the present study, we did not assess the molecular mechanisms of the immune potentiating function of CTB. However, our observation that simple mixing of Pvs25H-A with CTB did not produce a profound immune enhancement implies that its immunogenicity results from the antigen delivery, rather than a physiological cell activation, as occurs for CT. Further experiments are ongoing to characterize the immune potentiating function of CTB using the C-terminal 19-kDa fragment of merozoite surface protein 1 from *Plasmodium yoelii*. The results of these studies will help us judge whether CTB could contribute to a new platform technology for the design of s.c.-delivered subunit vaccines against infectious diseases such as malaria.

ACKNOWLEDGMENTS

We thank the staff of the Department of Entomology, Armed Forces Research Institute of Medical Sciences, Bangkok, Thailand, for their technical assistance.

This study was supported by the following grants: the Program of Founding Research Centers for Emerging and Reemerging Infectious Diseases from the Ministry of Education, Culture, Sports, Science and Technology, Japan (MEXT); Grants-in-Aid for Scientific Research (19406009 and 20590425) and Scientific Research on Priority Areas (21022034) from MEXT; a grant from The Okinawa Industry Promotion Public Corp. (Naha, Okinawa, Japan); and a Cooperative Research Grant from NEKKEN, 2010.

REFERENCES

1. **Arakawa, T., A. Komesu, H. Otsuki, J. Sattabongkot, R. Udomsangpetch, Y. Matsumoto, N. Tsuji, Y. Wu, M. Torii, and T. Tsuboi.** 2005. Nasal immunization with a malaria transmission-blocking vaccine candidate, Pfs25, induces complete protective immunity in mice against field isolates of *Plasmodium falciparum*. Infect. Immun. **73:**7375–7380.
2. **Arakawa, T., M. Tachibana, T. Miyata, T. Harakuni, H. Kohama, Y. Matsumoto, N. Tsuji, H. Hisaeda, A. Stowers, M. Torii, and T. Tsuboi.** 2009. Malaria ookinete surface protein-based vaccination via the intranasal route completely blocks parasite transmission in both passive and active vaccination regimens in a rodent model of malaria infection. Infect. Immun. **77:**5496–5500.
3. **Arakawa, T., T. Tsuboi, A. Kishimoto, J. Sattabongkot, N. Suwanabun, T. Rungruang, Y. Matsumoto, N. Tsuji, H. Hisaeda, A. Stowers, I. Shimabukuro, Y. Sato, and M. Torii.** 2003. Serum antibodies induced by intranasal immunization of mice with *Plasmodium vivax* Pvs25 co-administered with cholera toxin completely block parasite transmission to mosquitoes. Vaccine **21:**3143–3148.
4. **Arevalo-Herrera, M., C. Chitnis, and S. Herrera.** 2010. Current status of *Plasmodium vivax* vaccine. Hum. Vaccin. **6:**124–132.
5. **Bill and Melinda Gates Foundation.** 2009. Global health program. Bill and Melinda Gates Foundation, Seattle, WA. http://www.gatesfoundation.org/global-health/Documents/malaria-strategy.pdf.
6. **Birkett, A. J.** 2010. PATH Malaria Vaccine Initiative (MVI): perspectives on the status of malaria vaccine development. Hum. Vaccin. **6:**139–145.
7. **Carter, R.** 2001. Transmission blocking malaria vaccines. Vaccine **19:**2309–2314.
8. **Garcon, N., P. Chomez, and M. Van Mechelen.** 2007. GlaxoSmithKline adjuvant systems in vaccines: concepts, achievements and perspectives. Expert Rev. Vaccines **6:**723–739.
9. **Genton, B.** 2008. Malaria vaccines: a toy for travelers or a tool for eradication? Expert Rev. Vaccines **7:**597–611.
10. **Greenwood, B. M., D. A. Fidock, D. E. Kyle, S. H. Kappe, P. L. Alonso, F. H. Collins, and P. E. Duffy.** 2008. Malaria: progress, perils, and prospects for eradication. J. Clin. Invest. **118:**1266–1276.
11. **Harakuni, T., H. Sugawa, A. Komesu, M. Tadano, and T. Arakawa.** 2005. Heteropentameric cholera toxin B subunit chimeric molecules genetically fused to a vaccine antigen induce systemic and mucosal immune responses: a potential new strategy to target recombinant vaccine antigens to mucosal immune systems. Infect. Immun. **73:**5654–5665.
12. **Hisaeda, H., A. W. Stowers, T. Tsuboi, W. E. Collins, J. S. Sattabongkot, N. Suwanabun, M. Torii, and D. C. Kaslow.** 2000. Antibodies to malaria vaccine candidates Pvs25 and Pvs28 completely block the ability of *Plasmodium vivax* to infect mosquitoes. Infect. Immun. **68:**6618–6623.
13. **Holmgren, J., J. Adamsson, F. Anjuere, J. Clemens, C. Czerkinsky, K. Eriksson, C. F. Flach, A. George-Chandy, A. M. Harandi, M. Lebens, T. Lehner, M. Lindblad, E. Nygren, S. Raghavan, J. Sanchez, M. Stanford, J. B. Sun, A. M. Svennerholm, and S. Tengvall.** 2005. Mucosal adjuvants and anti-infection and anti-immunopathology vaccines based on cholera toxin, cholera toxin B subunit and CpG DNA. Immunol. Lett. **97:**181–188.
14. **Kaslow, D. C.** 1997. Transmission-blocking vaccines: uses and current status of development. Int. J. Parasitol. **27:**183–189.
15. **Kaslow, D. C., I. C. Bathurst, T. Lensen, T. Ponnudurai, P. J. Barr, and D. B. Keister.** 1994. *Saccharomyces cerevisiae* recombinant Pfs25 adsorbed to alum elicits antibodies that block transmission of *Plasmodium falciparum*. Infect. Immun. **62:**5576–5580.
16. **Kubler-Kielb, J., F. Majadly, Y. Wu, D. L. Narum, C. Guo, L. H. Miller, J. Shiloach, J. B. Robbins, and R. Schneerson.** 2007. Long-lasting and transmission-blocking activity of antibodies to *Plasmodium falciparum* elicited in mice by protein conjugates of Pfs25. Proc. Natl. Acad. Sci. U. S. A. **104:**293–298.
17. **Malkin, E. M., A. P. Durbin, D. J. Diemert, J. Sattabongkot, Y. Wu, K. Miura, C. A. Long, L. Lambert, A. P. Miles, J. Wang, A. Stowers, L. H. Miller, and A. Saul.** 2005. Phase 1 vaccine trial of Pvs25H: a transmission blocking vaccine for *Plasmodium vivax* malaria. Vaccine **23:**3131–3138.
18. **Mendis, K., B. J. Sina, P. Marchesini, and R. Carter.** 2001. The neglected burden of *Plasmodium vivax* malaria. Am. J. Trop. Med. Hyg. **64:**97–106.
19. **Miles, A. P., Y. Zhang, A. Saul, and A. W. Stowers.** 2002. Large-scale purification and characterization of malaria vaccine candidate antigen Pvs25H for use in clinical trials. Protein Expr. Purif. **25:**87–96.
20. **Peek, L. J., C. R. Middaugh, and C. Berkland.** 2008. Nanotechnology in vaccine delivery. Adv. Drug Deliv. Rev. **60:**915–928.
21. **Sachdeva, S., A. Mohmmed, P. V. Dasaradhi, B. S. Crabb, A. Katyal, P. Malhotra, and V. S. Chauhan.** 2006. Immunogenicity and protective efficacy

of *Escherichia coli* expressed *Plasmodium falciparum* merozoite surface protein-1_{42} using human compatible adjuvants. Vaccine **24:**2007–2016.
22. **Saxena, A. K., K. Singh, H. P. Su, M. M. Klein, A. W. Stowers, A. J. Saul, C. A. Long, and D. N. Garboczi.** 2006. The essential mosquito-stage P25 and P28 proteins from *Plasmodium* form tile-like triangular prisms. Nat. Struct. Mol. Biol. **13:**90–91.
23. **Suwanabun, N., J. Sattabongkot, T. Tsuboi, M. Torii, N. Maneechai, N. Rachapaew, N. Yim-amnuaychok, V. Punkitchar, and R. E. Coleman.** 2001. Development of a method for the in vitro production of *Plasmodium vivax* ookinetes. J. Parasitol. **87:**928–930.
24. **Targett, G. A., and B. M. Greenwood.** 2008. Malaria vaccines and their potential role in the elimination of malaria. Malar. J. **7**(Suppl. 1)**:**S10.
25. **Tsuboi, T., M. Tachibana, O. Kaneko, and M. Torii.** 2003. Transmission-blocking vaccine of vivax malaria. Parasitol. Int. **52:**1–11.
26. **van Ginkel, F. W., R. J. Jackson, Y. Yuki, and J. R. McGhee.** 2000. Cutting edge: the mucosal adjuvant cholera toxin redirects vaccine proteins into olfactory tissues. J. Immunol. **165:**4778–4782.
27. **Waitumbi, J. N., S. B. Anyona, C. W. Hunja, C. M. Kifude, M. E. Polhemus, D. S. Walsh, C. F. Ockenhouse, D. G. Heppner, A. Leach, M. Lievens, W. R. Ballou, J. D. Cohen, and C. J. Sutherland.** 2009. Impact of RTS,S/AS02(A) and RTS,S/AS01(B) on genotypes of *P. falciparum* in adults participating in a malaria vaccine clinical trial. PLoS One **4:**e7849.
28. **World Health Organization.** 2005. World health report. World Health Organization, Geneva Switzerland.
29. **Wu, Y., R. D. Ellis, D. Shaffer, E. Fontes, E. M. Malkin, S. Mahanty, M. P. Fay, D. Narum, K. Rausch, A. P. Miles, J. Aebig, A. Orcutt, O. Muratova, G. Song, L. Lambert, D. Zhu, K. Miura, C. Long, A. Saul, L. H. Miller, and A. P. Durbin.** 2008. Phase 1 trial of malaria transmission blocking vaccine candidates Pfs25 and Pvs25 formulated with montanide ISA 51. PLoS One **3:**e2636.
30. **Wu, Y., C. Przysiecki, E. Flanagan, S. N. Bello-Irizarry, R. Ionescu, O. Muratova, G. Dobrescu, L. Lambert, D. Keister, Y. Rippeon, C. A. Long, L. Shi, M. Caulfield, A. Shaw, A. Saul, J. Shiver, and L. H. Miller.** 2006. Sustained high-titer antibody responses induced by conjugating a malarial vaccine candidate to outer-membrane protein complex. Proc. Natl. Acad. Sci. U. S. A. **103:**18243–18248.

Editor: J. H. Adams

Vaccine 28 (2010) 6014–6020

Contents lists available at ScienceDirect

Vaccine

journal homepage: www.elsevier.com/locate/vaccine

Intranasal and intramuscular immunization with Baculovirus Dual Expression System-based Pvs25 vaccine substantially blocks *Plasmodium vivax* transmission

Andrew M. Blagborough[a,*], Shigeto Yoshida[b,**], Jetsumon Sattabongkot[c], Takafumi Tsuboi[d], Robert E. Sinden[a]

[a] Division of Cell and Molecular Biology, Department of Life Sciences, Sir Alexander Fleming Building, Imperial College London, Imperial College Road, London SW7 2AZ, UK
[b] Division of Medical Zoology, Department of Infection and Immunity, Jichi Medical University, Tochigi 329-0498, Japan
[c] Department of Entomology, Armed Forces Research Institute of Medical Sciences, Bangkok 10400, Thailand
[d] Cell-Free Science and Technology Research Center, Ehime University, Matsuyama, Ehime 790-8577, Japan

ARTICLE INFO

Article history:
Received 31 March 2010
Received in revised form 28 June 2010
Accepted 29 June 2010
Available online 14 July 2010

Keywords:
Malaria
Plasmodium vivax
Baculovirus
Transgenic

ABSTRACT

We have recently developed a new experimental vaccine vector system based on *Autographa californica* nucleopolyhedrosis virus (AcNPV) termed the "Baculovirus Dual Expression System", which drives expression of vaccine candidate antigens by a dual promoter that consists of tandemly arranged baculovirus-derived polyhedrin and mammalian-derived CMV promoters. The present study used this system to generate a *Plasmodium vivax* transmission-blocking immunogen (AcNPV-Dual-Pvs25). AcNPV-Dual-Pvs25 not only displayed Pvs25 on the AcNPV envelope, exhibiting aspects of its native three-dimensional structure, but also expressed appropriately immunogenic protein upon transduction of mammalian cells. Both intranasal and intramuscular immunization of mice with AcNPV-Dual-Pvs25 induced high Pvs25-specific antibody titres, notably of IgG1, IgG2a and IgG2b isotypes, indicating a mixed Th1/Th2 response. Importantly, sera obtained from subcutaneously immunized rabbits exhibited a significant transmission-blocking effect (96% reduction in infection intensity, 24% reduction in prevalence) when challenged with human blood infected with *P. vivax* gametocytes using the standard membrane feeding assay. Additionally, active immunization (both intranasal and intramuscular routes) of mice followed by challenge using a transgenic *P. berghei* line expressing Pvs25 in place of native Pbs25 and Pbs28 (clone Pvs25DR3) demonstrates a strong transmission-blocking response, with a 92.1% (intranasal) and 83.8% (intramuscular) reduction in oocyst intensity. Corresponding reductions in prevalence of infection were observed (88.4% and 75.5% respectively). This study offers a novel tool for the development of malarial transmission-blocking vaccines against the sexual stages of the parasite, using the Baculovirus Dual Expression System that functions as both a subunit, and DNA based vaccine.

1. Introduction

Malaria is a serious, acute and sometimes relapsing disease, caused by protozoan parasites of the genus *Plasmodium*. It is responsible for high morbidity and mortality in tropical and subtropical regions, causing approximately 1 million deaths per year, the majority of whom are African children under the age of five [25]. Given the complex life cycles of the different plasmodial species and the distinct host immune responses to each developmental stage, *Plasmodium* provides many potential targets for the development of prophylactic vaccines against the parasite.

An anti-malarial transmission-blocking vaccine (TBV) that prevents fertilization and/or ookinete/oocyst development within the mosquito is an attractive strategy to limit the transmission of malaria. The ookinete proteins Pvs25 and Pvs28 which are expressed on the surface of the sexual and early sporogonic forms of *Plasmodium vivax* are presently lead targets for the development of a *P. vivax* TBV [15–18]. A variety of expression vectors (e.g., *Escherichia coli*, *Pichia pastoris* and DNA) have been used to express Pvs25 protein which has been administered alone or in combination with adjuvants (e.g., Freund's adjuvant, aluminum hydroxide and cholera toxin) [19,20,26,33,34]. To date these studies suggest that the recombinant protein currently requires both not only linear, but conformation dependent epitopes, and a strong adjuvant to induce transmission-blocking antibodies. Phase I human trials with a clinical-grade recombinant Pvs25 produced by *P. pastoris* administered with an alum adjuvant produced antibodies that inhibit transmission of the parasite by ~80% (intensity) and 20–30% (prevalence) [19].

* Corresponding author at: Imperial College Road, London SW7 2AZ, UK. Tel.: +44 0 20 7594 5350.
** Corresponding author at: 3311-1 Yakushiji, Shimotsuke, Tochigi 329-0498, Japan. Tel.: +81 285 58 7339; fax: +81 285 44 6489.
E-mail addresses: andrew.blagborough@imperial.ac.uk (A.M. Blagborough), shigeto@jichi.ac.jp (S. Yoshida).

0264-410X/$ – see front matter © 2010 Elsevier Ltd. All rights reserved.
doi:10.1016/j.vaccine.2010.06.100

To improve the safety and efficacy of current Pvs25-based TBV candidates, new vaccine vehicles and/or delivery systems (e.g., needle- and adjuvant-free, long-lasting and cost-effective) need to be considered. In addition, a suitable small-animal model for the *in vivo* assessment of *P. vivax* TBV-induced functional immune responses might provide a useful tool for evaluating its TBV efficacy before proceeding to human clinical trials. Recently, we have developed a new vaccine vector system based on the baculovirus *Autographa californica* nucleopolyhedrosis virus (AcNPV) termed the "Baculovirus Dual Expression System", which drives expression of vaccine candidate antigens by a dual promoter that consists of tandemly arranged baculovirus-derived polyhedrin and mammalian-derived CMV promoters. It has been shown that AcNPV, an enveloped double-stranded DNA virus that naturally infects insects, possesses strong adjuvant properties that can activate dendritic cell-mediated innate immunity through MyD88/TLR9-dependent and -independent pathways [30]. When applied to *P. berghei* circumsporozoite protein (PbCSP) as a model for malaria pre-erythrocytic stage vaccine, this immunogen elicited high PbCSP-specific antibody titres and PbCSP-specific $CD8^+$ T-cell responses without extraneous immunological adjuvants in mice, and conferred complete protection against sporozoite challenge [8]. The Baculovirus Dual Expression System therefore constitutes an innate immunostimulating complex, and functions as a subunit and DNA vaccine that generates strong humoral and cellular immune responses. In addition, the AcNPV-based vaccine has another great potential for adjuvant-free intranasal (i.n.) administration. For blood-stage malaria vaccine development, we have also shown that i.n. immunization with AcNPV-based vaccine expressing *P. yoelii* merozoite surface protein 1 19 kDa fragment ($PyMSP1_{19}$) induced not only strong systemic humoral immune responses with high titre of $PyMSP1_{19}$-specific antibody but also natural boosting of $PyMSP1_{19}$-specific antibody responses at a short time following challenge, and conferred complete protection [28].

Here we evaluate a second-generation transmission-blocking Pvs25 immunization protocol based on the Baculovirus Dual Expression System (AcNPV-Dual-Pvs25). We show that the AcNPV-Dual-Pvs25 elicits highly effective Pvs25-specific humoral immune responses, and confers significant transmission-blocking activity, assessed by the standard membrane feeding assay (SMFA) on peripheral blood from *P. vivax* infected patients, and by active immunization of mice challenged with *P. berghei* expressing Pv25 (Pvs25DR3), which has been specifically generated as a murine model for the *in vivo* assessment of Pvs25-based TBV-induced functional immune responses [12].

The data reported here demonstrates the successful implementation of the Baculovirus Dual Expression System using both i.n. and intramuscular (i.m.) methods of delivery, giving equivalent responses for each method of immunization. Our results show that the Baculovirus Dual Expression System provides a simple, non-toxic, safe and adjuvant-free vaccine delivery platform, and as such could be considered as a powerful tool for the development of future TBVs against *Plasmodium* spp.

2. Materials and methods

2.1. Cell lines, mice and parasites

Sf9 cells were maintained at 27 °C in SF900-II medium (Invitrogen, San Diego, CA) supplemented with antibiotics. HepG2 cells were maintained at 37 °C in Dulbecco's modified Eagle's medium (Invitrogen) supplemented with 10% (v/v) heat-inactivated fetal bovine serum, 2 mM L-glutamine, and antibiotics. Female BALB/c or Theiler's Original (TO) mice, 7–8 weeks of age at the start of the experiment, were purchased from Harlan (UK). *P. berghei* clones ANKA 2.34 and Pvs25DR3 [12] were used for challenge infections. General parasite maintenance was carried out as described previously [24].

2.2. Recombinant baculovirus

The DNA sequence corresponding to amino acids Ala_{23}-Leu_{195} of Pvs25 (*P. vivax* Salvador I strain) was amplified from pEU3-Pvs25 [27] using the primers pPvs25-F1 (5′-GAATTCATGGCTAGCGCCGTCACGGTAGACACC-3′) and pPvs25-R1 (5′-CCCGGGGCCCAAGGCATACATTTTTCTCTTT-3′). The PCR product was ligated into the *Eco*RI/*Sma*I sites of pTriEx–PbCSP–gp64 [8] to construct a baculovirus transfer vector, pTriEx–Pvs25–gp64 (Fig. 1). The recombinant baculovirus AcNPV-Dual-Pvs25 was generated in Sf9 cells by co-transfection of the recombinant transfer plasmids pTriEx–Pvs25–gp64, with BacVector-2000 DNA (Novagen), according to the manufacturer's protocol. Purification of viral particles was performed as described previously [8]. The purified baculovirus particles were free of endotoxin (<0.01 endotoxin units/10^9 PFU), as determined by the Endospecy® endotoxin measurement kit (Seikagaku Co., Tokyo, Japan).

2.3. Recombinant proteins

A 0.5-kb fragment of the *Pvs25* gene (encoding amino acids 23–159) was excised from pTriEx–Pvs25–gp64 by digestion with *Eco*RI and *Sma*I, and inserted into the *Eco*RI/*Sma*I sites of pGEX-4T-1 (GE Healthcare) to construct the recombinant expression plasmid, pGEX-Pvs25. Recombinant Pvs25, created as a fusion protein with glutathione S-transferase (GST-Pvs25), was expressed in *E. coli* and purified using a GST affinity column (GE Healthcare) as described previously [1]. Resultant protein was used as an immunogen for vaccination of mice and as antigen for isotype analysis.

2.4. Western blotting and indirect immunofluorescence assay (IFA)

Western blotting was carried out as described previously [2]. HepG2 cells were seeded at a density of 5×10^4 cells/well in collagen-type-I-coated eight-well chamber slides (BD Biosciences) and transduced with purified baculovirus particles at an m.o.i. of 10. After 48 h incubation, cells were fixed for 15 min in acetone/methanol [6,4] at −20 °C, and incubated with anti-Pvs25 mAb N1-1H10 (MR4, Manassas, VA) and then with FITC-conjugated goat anti-mouse IgG (Biosource International, Camarillo, CA).

For preparation of *P. vivax* ookinetes, peripheral blood was collected in heparinized syringes under written informed consent from patients who attended malaria clinics within the Mae Sod district in the Tak province of northwestern Thailand. The use of all human materials in this study was reviewed and approved by the Institutional Ethics Committee of the Thai Ministry of Public Health and the Human Subjects Research Review Board of the Walter Reed Army Institute of Research, USA. For IFA, cultured *P. vivax* parasite preparations rich in zygotes and small numbers of ookinetes were spotted on slides and fixed with acetone. Sera obtained from immunized mice were tested by IFA on the fixed parasite material. To confirm the position of all parasites in the IFA, the slides were stained with DAPI (4′,6-diamidino-2-phenylindole) (Wako Pure Chemical, Osaka, Japan). Bound antibodies and labeled nuclei were recorded by confocal scanning laser microscopy (LSM5 PASCAL; Carl Zeiss MicroImaging, Thornwood, NY).

2.5. Immunization

Mice were immunized four times at 3-week intervals with 5×10^7 PFU of AcNPV-Dual-Pvs25 either by the i.m. or i.n. routes.

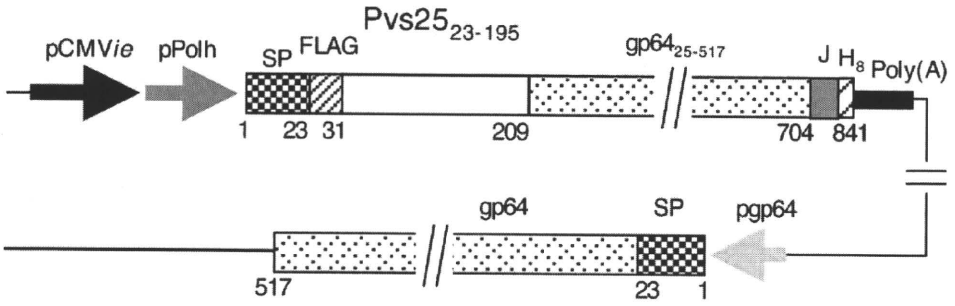

Fig. 1. Schematic representation of AcNPV-Dual-Pvs25 genome structure. A gene cassette that consisted of the gp64 signal sequence (SP), the *Pvs25* gene ($Pvs25_{25-195}$) fused to the N terminus of the AcNPV major envelope protein *gp64* gene ($gp64_{25-517}$), and the rabbit β-globlin poly(A) signal [poly(A)]. Expression of the gene cassette was driven by a dual promoter that consisted of the CMV immediate early enhancer/promoter (pCMV*ie*) and the polyhedrin promoter (pPolh). AcNPV-Dual-Pvs25 also possessed the endogenous *gp64* gene. Numbers indicate the amino acid positions of Pvs25–gp64 fusion protein and endogenous gp64. FLAG, FLAG epitope tag; $Pvs25_{25-195}$, Pvs25 corresponding to amino acids 25–195; $gp64_{25-517}$, gp64 corresponding to amino acids 25–517; J, junction consisting of 29 unrelated amino acid residues; H8, His-tag; pgp64, gp64 promoter.

For i.n. immunization, a total of 50 μl, divided into three doses delivered at 5-min intervals, was inoculated dropwise with a 20 μl pipette. As a comparative (negative) control, mice were immunized i.n. with 1×10^8 PFU of AcNPV-CMV-EGFP. Sera were collected two weeks after the final immunization prior to infection with *P. berghei* (either ANKA 2.34 or Pvs25DR3) to evaluate anti-Pvs25 response by ELISA. Immunized mice were kept for a total of 5 months following final immunization to quantify immune response over a longer time period. Serum was harvested from each mouse on a monthly basis, and ELISA performed as described below.

To prepare antibodies for use in standard membrane feeding assays using vivax patient blood, rabbits were immunized subcutaneously three times at 3-week intervals with 1×10^8 PFU of AcNPV-Dual-Pvs25. Two weeks after the final immunization, sera were collected and IgG purified using HiTrap™ Protein G HP chromatography (GE Healthcare) together with pre-immune rabbit sera.

2.6. ELISA for antibody titres and isotypes

Sera obtained from immunized mice were collected by tail bleeds prior to challenge. For some mice, sera were also collected periodically after final immunization. ELISA plates pre-coated with 100 ng/well GST-Pvs25 were incubated with serial dilutions of sera. Specific IgGs were detected using HRP-conjugated goat anti-mouse IgG (H + L) (Bio-Rad, Hercules, CA). For isotype determination, HRP-conjugated rabbit anti-mouse IgG1, IgG2a, IgG2b, and IgG3 (Zymed Laboratories, San Francisco, CA) antibodies were used. The plates were developed with peroxidase substrate solution [H_2O_2 and 2,2′-azino-bis(3-ethylbenzthiazoline-6-sulphonic acid)]. The OD at 414 nm of each well was measured using a plate reader. Endpoint titres were expressed as the reciprocal of the highest sample dilution for which the OD was equal or greater than the mean OD of non-immune control sera.

2.7. Transmission-blocking assay (standard membrane feeding assay)

Peripheral blood was collected from four volunteer patients infected only with *P. vivax* as described above. Purified anti-AcNPV-Dual-Pvs25 rabbit IgG was diluted (1-, 4- and 16-fold) with IgG from pre-immune rabbits, then 75 μl of each rabbit IgG mixture was mixed with 105 μl of heat-inactivated normal human AB serum prepared from malaria naive Thai donors. Diluted IgG was mixed with *P. vivax*-infected blood cells (1:1, v/v ratio) and incubated for 15 min at room temperature. The mixture was placed in a membrane feeding apparatus at 37 °C. *Anopheles dirus* A mosquitoes (Bangkok colony, Armed Forces Research Institute of Medical Sciences) were allowed to feed for 30 min. Unfed mosquitoes were removed after blood feeding, and fully engorged mosquitoes were maintained on 10% sucrose for seven days. For each diluted IgG, at least 20 mosquitoes were dissected and analyzed by staining with 0.5% mercurochrome and subsequent microscopy to count the number of oocysts that developed on the mosquito midguts.

2.8. Transmission-blocking assay (active immunization)

In three separate experiments, mice immunized i.m. or i.n. with AcNPV-Dual-Pvs25 were divided into two groups (three mice per group), PH treated, and three days later infected i.p. with 10^6 parasites of *P. berghei* ANKA 2.34 or *P. berghei* Pvs25DR3. As a negative control, mice were immunized i.n. with AcNPV-CMV-EGFP, divided into two groups and infected as above. Three days post-infection, starved *A. stephensi* mosquitoes were allowed to feed on the infected mice. In all pots, >50 fed mosquitoes were fed per mouse. 24 h after feeding, mosquitoes were briefly anesthetized with CO_2, and unfeds removed. Mosquitoes were then maintained on fructose [8% (w/v) fructose, 0.05% (w/v) *p*-aminobenzoic acid] at 19–22 °C and 50–80% relative humidity. Day 10 post-feeding, mosquito midguts were dissected, and oocyst prevalence and intensity recorded. All care and handling of animals was in accordance with the Guidelines for Animal Care and Use prepared by Jichi Medical University and Imperial College London.

2.9. Statistical analyses

Statistical analysis was performed with Graphpad Prism Software (Graphpad Software Inc.). For the membrane feeding assay, The Kruskal–Wallis test was used to examine the difference in oocyst counts per mosquito between pre-immune IgG and immune IgG groups. For long-term anti-Pvs25 ELISA responses, significant variations of titres over time were evaluated using Spearman's rank correlation ($p < 0.05$). For active immunization, significance was assessed using Mann–Whitney *U* test (to examine the difference in oocyst counts per mosquito between AcNPV-Dual-Pvs25 or AcNPV-CMV-EGFP immunized groups) and the Fisher's exact probability test (to examine the difference in infection prevelance between AcNPV-Dual-Pvs25 or AcNPV-CMV-EGFP immunized groups) *P* values less than 0.05 were considered statistically significant.

3. Results

3.1. Construction of baculovirus-based Pvs25 vaccine

To examine the expression of conformation-dependent epitopes, AcNPV-Dual-Pvs25 viral particles were analyzed by

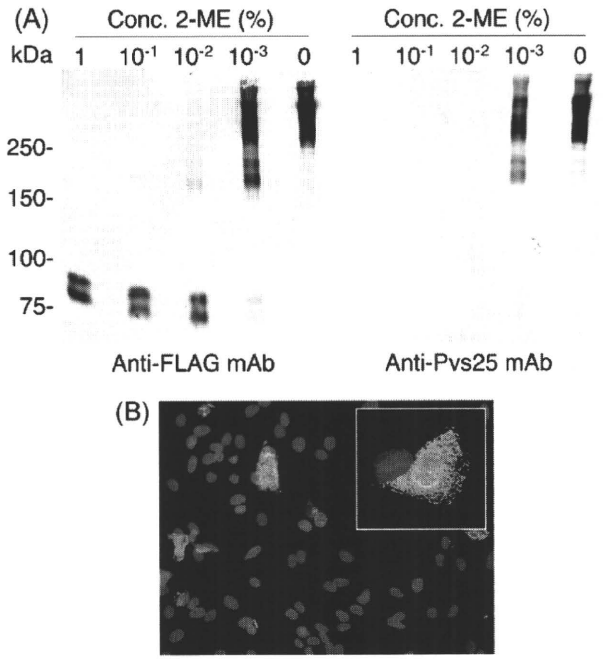

Fig. 2. Expression of Pvs25–gp64 fusion protein. (A) Western blotting of AcNPV-Dual-Pvs25 in the presence of various concentrations of 2-ME. AcNPV-Dual-Pvs25 was treated with the loading buffer containing descending concentrations of 2-ME. Reactivity of $Pvs25_{25-195}$ fusion protein was examined using either anti-FLAG mAb or anti-Pvs25 mAb, N1-1H10. The concentrations of 2-ME are shown above the gel. (B) *In vitro* expression analysis of Pvs25 by transducing AcNPV-Dual-Pvs25 in mammalian cells. HepG2 cells were transduced with AcNPV-Dual-Pvs25 at an m.o.i. of 10. Forty-eight hours later, cells were fixed with 5% paraformaldehyde followed by permeabilization with 0.1% Triton X in PBS, and incubated with anti-Pvs25 mAb 1H10. Bound antibodies were detected by FITC-labeled anti-mouse IgG by fluorescence microscopy (green). Cell nuclei were visualized by DAPI staining (blue). Original magnification, ×400.

Western blotting in the absence or presence of 10^{-3}% to 1% 2-mercaptoethanol (2-ME) (Fig. 2A). Anti-FLAG mAb, which recognizes a linear epitope within the N-terminal tag, reacted with doublet bands at all 2-ME concentrations, with relative molecular masses (M_r) of 80 and 90 kDa. The 80 kDa band corresponded to the predicted M_r of the Pvs25–gp64 fusion protein (Fig. 2A, left panel). We hypothesise the 90 kDa band may have resulted from post-translational modification within the insect cells. When 2-ME is added at concentrations above 10^{-3}%, recognition by anti-Pvs25 mAb N1-1H10, which has previously been shown to recognize a conformation-dependent epitope [29], is not detectable. In contrast, reducing of the concentration of 2-ME to below 10^{-3}% increased the reactivity of Pvs25–gp64 fusion protein with the mAb (Fig. 2A, right panel). These results suggest that the Pvs25–gp64 fusion protein on the virus envelope retains components of the three-dimensional structure of native Pvs25 protein, important to antibody recognition.

We also examined by IFA the ability of AcNPV-Dual-Pvs25 to drive Pvs25 expression in mammalian cells. Strong immunofluorescence signals were detected with N1-1H10 mAb in HepG2 cells infected with AcNPV-Dual-Pvs25 48 h after transfection (Fig. 2B). Thus AcNPV-Dual-Pvs25 not only expressed appropriately folded Pvs25 on viral particles, but also in mammalian cells.

3.2. Immunization with AcNPV-Dual-Pvs25 induces high Pvs25-specific antibody titres

I.n. and i.m. immunization with AcNPV-Dual-Pvs25 induced high antibody titres (>1:15,000) (Fig. 3A). Pvs25 antibodies were predominately IgG1, IgG2a and IgG2b (IgG1:IgG2a ratio ≅0.12 and 0.29 for i.m. and i.n. immunizations, respectively), indicating a mixed Th1/Th2-type immune response. IgG2b, which is inducible by mucosal immunization, was significantly higher in the i.n. group than the i.m. group. As demonstrated by the IFA test, these immune sera strongly reacted with Pvs25 in its native location on the parasite surface, circumferential staining of the *P. vivax* retort-form ookinete was prominent (Fig. 3B). Pvs25-specific antibody titres in sera obtained from both the i.m. and i.n. AcNPV-Dual-Pvs25 groups were sustained without any significant reduction over 5 months following the final immunization (Fig. 4).

3.3. Evaluation of transmission-blocking activity (SMFA)

Following subcutaneous immunization with AcNPV-Dual-Pvs25, IgG purified from immune rabbit serum reduced the intensity and prevalence of oocyst infection on the mosquito midgut profoundly (Fig. 5), in a dose-dependent manner. At an immune IgG concentration of 0.17 mg/ml, the mean intensity observed was 73.9 oocysts/midgut, and at 2.67 mg/ml, intensity was reduced to just 1.5 oocysts/midgut (a 98% inhibition of intensity when compared to pre-immune IgG at 2.67 mg/ml). Prevalence of infection was reduced by 70% from 94% in the pre-immune control, to give an overall reduction of 25.5% (with respect to pre-immune IgG). At lower concentrations of immune IgG tested, no significant reduction of prevalence was observed.

3.4. Evaluation of transmission-blocking activity (in vivo evaluation)

To examine transmission blockade *in vivo*, immunized mice were infected with transgenic *P. berghei* expressing Pv25 (Pvs25DR3), *A. stephensi* mosquitoes were fed directly on the immunized and challenged hosts (Table 1). AcNPV-Dual-Pvs25 was administered either by i.m. or i.n. route into six mice each. Six control mice were also immunized i.n. with AcNPV-CMV-EGFP as a negative control. For each immunization method, three mice were challenged with *P. berghei* ANKA 2.34 (to determine whether there was a direct but unexpected anti-*P. berghei* response), and three were immunized with *P. berghei* Pvs25DR3. WT *P. berghei* 2.34 does not express Pvs25, and any TB effect observed would be due to non-specific phenomenon. *P. berghei* Pvs25DR3 expresses Pvs25 on the zygote and ookinete surface [12]. Mosquitoes that fed on control (AcNPV-CMV-EGFP) mice immunized by the intranasal route displayed an, average intensity of infection of 2.16 oocysts/midgut (±S.E.M.), whereas following mucosal delivery of AcNPV-Dual-Pvs25 and subsequent challenge, the average intensity was significantly reduced to 0.17 oocysts/midgut (±S.E.M.). Following intramuscular delivery, intensity was 0.25 oocysts/midgut (±S.E.M.); thus achieving a 92.1% and an 88.4% inhibition of intensity of infection with intranasal and intramuscular deliveries, respectively. Prevalence was similarly reduced, by 83.8% and 75.5% respectively.

4. Discussion

The Baculovirus Dual Expression System aims to facilitate the development of multifunctional vaccines capable of inducing strong humoral and cellular immune responses without the need for extraneous immunological adjuvants. In the present study, we applied this system to generation of a novel *P. vivax* TBV (AcNPV-Dual-Pvs25), which possesses a single gene cassette that consists of the Pvs25–gp64 fusion gene under the CMV-polyhedrin dual promoter. AcNPV-Dual-Pvs25 not only displayed Pvs25 on the viral envelope but also expressed following transduction of mammalian cells. Immunization of mice with AcNPV-Dual-Pvs25 induced high Pvs25-specific antibody titres with predominant IgG1, IgG2a and

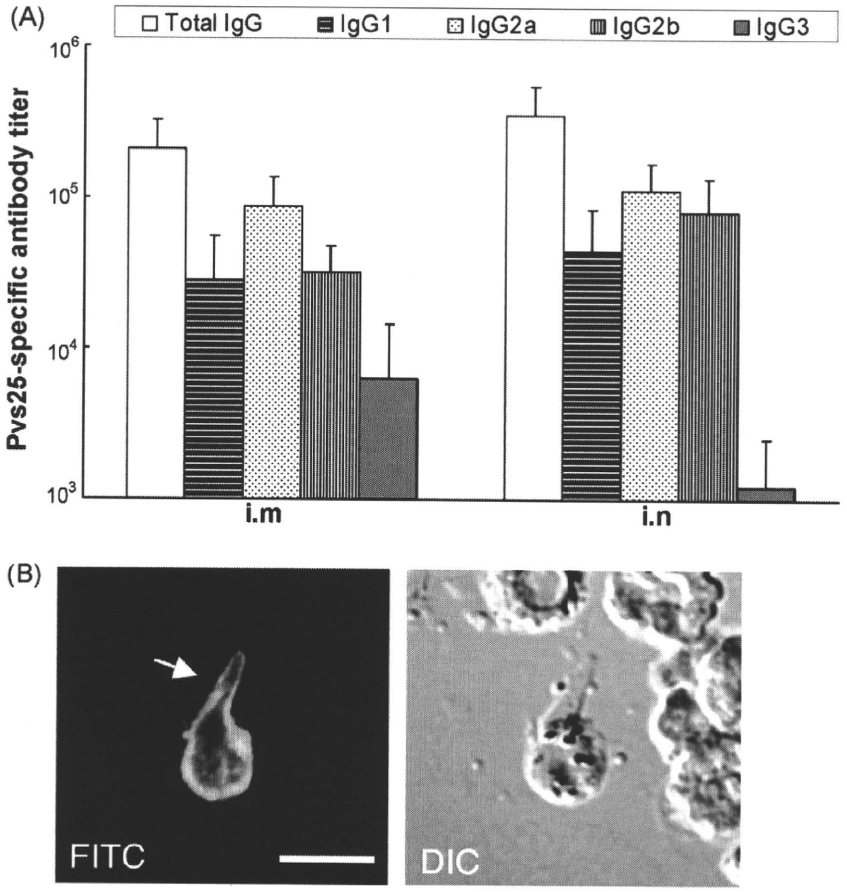

Fig. 3. Pvs25-specific antibody responses. Sera were collected from individual mice (6 mice/group) three weeks after the final immunization. (A) The individual sera were tested for total IgG, IgG1, IgG2a, IgG2b and IgG3 specific for Pvs25 by ELISA. The data represent one of two experiments, which had similar results. Data are the mean ± S.E.M. of groups. Significant differences of total IgG titres between different groups were evaluated using the two-tailed Fisher's exact probability test. *, $p < 0.01$. (B) Confocal fluorescence microscopy of sera obtained from mice immunized with AcNPV-Dual-Pvs25. The entire surface of cultured retorts/zygotes was clearly stained (green) by serum (1:500 dilution) obtained from a mouse immunized i.n. with AcNPV-Dual-Pvs25. Cell nuclei were visualized by blue DAPI staining (arrow) (immunofluorescence assay [IFA]). Right panel represents image obtained by differential interference contrast (DIC) microscopy. Scale bar, 10 μm.

IgG2b isotypes, indicating induction of both a mixed Th1/Th2 response.

We evaluated the transmission-blocking immunogenicity of AcNPV-Dual-Pvs25 using two methods. One was SMFA on peripheral blood from *P. vivax* infected patients. It has widely been accepted that malaria transmission-blocking immunity is mediated by antibodies that inhibit parasite development in the mosquito midgut [15,23,31,32]. The SMFA has provided valuable insights into functional transmission-blocking activities of sera from immunized animals. However, blood from *P. vivax*-infected patients as a source of SMFA is an unpredictable, and uncontrollable source of parasites and useful *in vitro* gametocyte culture has not been established. The other method was active immunization of mice followed by challenge with transgenic *P. berghei* Pvs25DR3. Compared with SMFA, active immunization/challenge method can assess the *in vivo* transmission-blocking potential of all immune factors including not only antibodies but also cytokine, complement and antibody-dependent cell cytotoxity. The approach of using transgenic rodent malarial parasites to assess the immune system's response to targets from a human malarial parasite has been described in previous studies [12–14]. Whilst the infectivity of all Pvs25DR3 transgenic lines tested to date is low compare to WT *P. berghei*, oocyst intensities are close to that seen *in vivo* for both *P. vivax* (and *P. falciparum*), and provide a very sensitive context to measure any transmission-blocking effect. Importantly, the transmission-blocking assays used clearly demonstrated that immunization with AcNPV-Dual-Pvs25 induced a strong transmission-blocking response, namely >90% reduction in oocyst number, and a corresponding fall in prevalence of 25.5% (SMFA) and 83.8% (i.n.)/75.5% (i.m.) (active immunization). These results provide support for this novel strategy for the delivery of a malarial TBV.

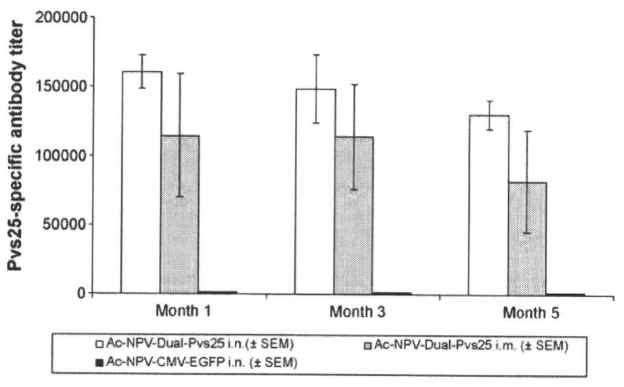

Fig. 4. Long-term ELISA titres following immunization with AcNPV-Dual-Pvs25. Sera were collected from individual mice three weeks following final immunization, and then at monthly intervals for 5 months. Six mice were examined for each immunogen. The individual sera were tested for total IgG specific for recombinant Pvs25 by ELISA. Samples shown are mean titres observed from six mice. Error bars show S.E.M. Significant variations of titres over time were evaluated using Spearman's rank correlation ($p < 0.05$). No statistically significant variation was observed in groups over 5 months.

Table 1
Evaluation of transmission-blocking activity by active immunization.

		Mean intensity (±S.E.M.)	Mean prevalence (% mosquitoes infected) (±S.E.M.)
AcNPV-Dual-Pvs25 immunized mice—i.n. delivery			
Mice 1–3: Pvs25DR3 challenged (±S.E.M.)		0.17 (0.1)	10.7 (3.1)
Mice 4–6: WT 2.34 challenged (±S.E.M.)		112.9 (8.43)	93.8 (3.46)
AcNPV-Dual-Pvs25 immunized mice—i.m. delivery			
Mice 7–9: Pvs25DR3 challenged (±S.E.M.)		0.25 (0.06)	16.2 (1.27)
Mice 10–12: WT 2.34 challenged (±S.E.M.)		88.8 (11.2)	89.6 (4.7)
AcNPV-CMV-EGFP immunized mice—i.n. delivery (negative control)			
Mice 13–15: Pvs25DR3 challenged (±S.E.M.)		2.16 (0.2)	66(4.23)
Mice 16–18: WT 2.34 challenged (±S.E.M.)		87.41 (15.6)	82.6 (10.9)
		Mean change in intensity	Mean change in prevalence
Overall Transmission blockade in AcNPV-Dual-Pvs25 immunised mice			
I.n.	Pvs25DR3	−92.10%[a]	−83.80%[b]
	P. berghei 2.34	+29.70%	+13.60%
I.m.	Pvs25DR3	−88.40%[a]	−75.50%[b]
	P. berghei 2.34	+1.60%	+8.50%

Mice were immunized four times with AcNPV-Dual-Pvs25 (i.m. and i.n.) or AcNPV-CMV-EGFP (i.n. only, negative control). Three groups of immunized mice were sub-divided into two groups, each containing three mice. Each group was then and challenged with WT *P. berghei* 2.34 (3 mice) or *P. berghei* Pvs25DR3 (3 mice), and used to assess transmission to mosquitoes via direct gametocyte feed. 10^6 parasites were injected per mouse. Mosquito midguts were dissected 10–12 days post feed. Mean intensities and prevalence were calculated from triplicate mice. Overall transmission blockade (in terms of both infection intensity and prevelance) was calculated by comparison to AcNPV-CMV-EGFP immunized mice. Significance was assessed using Mann–Whitney *U* test (to examine the difference in oocyst counts per mosquito between AcNPV-Dual-Pvs25 or AcNPV-CMV-EGFP immunized groups) and the Fisher's exact probability test (to examine the difference in infection prevelance between AcNPV-Dual-Pvs25 or AcNPV-CMV-EGFP immunized groups) ($p < 0.05$). Following challenge with WT *P. berghei* 2.34, no significant change in either intensity or prevalence was observed with either intranasal or intramuscular immunization. Significant inhibition was only observed following challenge with Pvs25DR3.

[a] $P < 0.05$, Mann–Whitney *U* test.

[b] $P < 0.05$, Fisher's exact probability test.

Mucosal vaccines have several attractive features compared with parenteral vaccines (e.g., safety, cost-effectiveness and ease of administration), but studies on their use have been limited almost exclusively to protection against mucosally transmitted pathogens. We provide evidence that i.n. immunization is a feasible alternative for preventing malaria, which is transmitted through non-mucosal routes. Compared with i.m. immunization, i.n. immunization led to higher Pvs25-specific antibody titres and potent transmission-blocking activity (i.n.:i.m.; intensity = 92.1%:88.4%, prevalence = 83.8%:75.5%). These results are consistent with our previous work showing that intranasal immunization with the baculovirus-based vaccine induced strong systemic humoral immune responses with high titres of antigen-specific antibodies and conferred complete protection against malaria blood-stage challenge [8,9,28]. It has previously been reported that intranasal immunization with recombinant Pvs25, using cholera toxin (CT) as an adjuvant, induced a systemic immune response with transmission-blocking activity [21]. Additionally, the mucosal immunogenicity and protective efficacy of recombinant Pfs25 and Pys25 have been thoroughly described [10,11]. CT, whilst a strong immune potentiator [10,11,21], which can induce immunological memory against heterologous antigens in a rodent model; however, it is precluded from clinical use due to its enterotoxicity and potential hazardous effects on olfactory nerves [22]. In contrast, a baculovirus-based delivery system may offer an attractive immunization method, as AcNPV exhibits low cytotoxicity and is incapable of replication in mammalian cells [8,9].

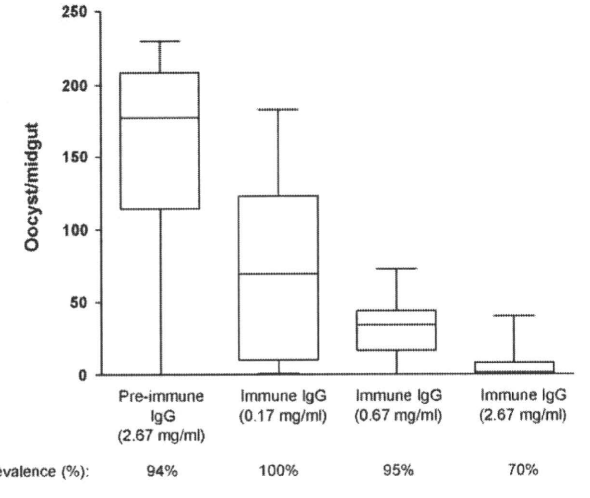

Fig. 5. Transmission-blocking efficacy against Thai *P. vivax* isolates by membrane feeding assay. Rabbits were immunized subcutaneously with AcNPV-Dual-Pvs25 vaccine. The purified rabbit IgG was evaluated by membrane feeding of *P. vivax*-infected blood from patients in Thailand. The IgG effectively inhibited oocyst formation in the mosquito midguts in a dose-dependent manner. Experiments were performed using blood from four volunteers naturally infected with *P. vivax*. The data presented was obtained from one volunteer. Data are expressed as the median numbers of oocysts per mosquitoes (lines in boxes), quartiles (boxes), and ranges (lines above and below boxes). Stastistically significant differences in oocyst counts per mosquito between pre-immune IgG and immune IgG groups were confirmed by the Kruskal–Wallis test ($P < 0.0001$).

Anti-malarial transmission-blocking vaccines based on the surface of the sexual and other sporogonic stages of *Plasmodium* inhibit further development of the parasite within the mosquito host, and have a significant potential to reduce malarial transmission in endemic areas. The data described here adds to previously presented data showing the significant potential of the baculovirus dual expression system against the blood stages of the parasite [8,9,28], but also demonstrates clearly its ability to induce antibodies against the ookinete surface protein Pvs25, and to elicit a transmission-blocking immune response against the *P. vivax* isolates from endemic areas, and a transgenic rodent malaria parasite model in preliminary studies.

Acknowledgments

We would like to thank Hitomi Araki for excellent assistance with the ELISAs and handling of the mice. We also thank Ken

Baker and Mark Tunnicliff for mosquito rearing (Imperial College, London). This work was supported by grants from the Ministry of Education, Culture, Sports and Science of Japan (21390126) (Jichi Medical University), and Biomalpar, Transmolbloc and BBSRC (award number LDAD_P15820) (Imperial College, London).

References

[1] Daly TM, Long CA. A recombinant 15-kilodalton carboxyl-terminal fragment of *Plasmodium yoelii yoelii* 17XL merozoite surface protein 1 induces a protective immune response in mice. Infect Immun 1993;61:2462–7.
[2] Davies AH. "Baculophage": a new tool for protein display. Biotechnology (N Y) 1995;13:1046.
[4] Jin R, Lv Z, Chen Q, Quan Y, Zhang H, Li S, et al. Safety and immunogenicity of H5N1 influenza vaccine based on baculovirus surface display system of *Bombyx mori*. PLoS ONE 2008;3:e3933.
[6] Matsuura Y, Possee RD, Overton HA, Bishop DH. Baculovirus expression vectors: the requirements for high level expression of proteins, including glycoproteins. J Gen Virol 1987;68(Pt 5):1233–50.
[8] Yoshida S, Kawasaki M, Hariguchi N, Hirota K, Matsumoto M. A baculovirus dual expression system-based malaria vaccine induces strong protection against *Plasmodium berghei* sporozoite challenge in mice. Infect Immun 2009;77:1782–9.
[9] Yoshida S, Kondoh D, Arai E, Matsuoka H, Seki C, Tanaka T, et al. Baculovirus virions displaying *Plasmodium berghei* circumsporozoite protein protect mice against malaria sporozoite infection. Virology 2003;316:161–70.
[10] Arakawa T, Tachibana M, Miyata T, Harakuni T, Kohama H, Matsumoto Y, et al. Malaria ookinete surface protein-based vaccination via the intranasal route completely blocks parasite transmission both in passive and active vaccination regimes in a rodent malaria infection model. Infect Immun 2009. E-pub ahead of print 14th Sep.
[11] Arakawa T, Komesu A, Otsuki H, Sattabongkot J, Udomsangpetch R, Matsumoto Y, et al. Nasal immunization with a malaria transmission-blocking vaccine candidate, Pfs25, induces complete protective immunity in mice against field isolates of *Plasmodium falciparum*. Infect Immun 2005;73(11):7375–80.
[12] Ramjanee S, Robertson JS, Franke-Fayard B, Sinha R, Waters AP, Janse CJ, et al. The use of transgenic *Plasmodium berghei* expressing the *Plasmodium vivax* antigen P25 to determine the transmission-blocking activity of sera from malaria vaccine trials. Vaccine 2007;25(January (5)):886–94.
[13] Mlambo G, Maciel J, Kumar N. Murine model for assessment of *Plasmodium falciparum* transmission-blocking vaccine using transgenic *Plasmodium berghei* parasites expressing the target antigen Pfs25. Infect Immun 2008;76(May (5)):2018–24.
[14] Kumar KA, Oliveira GA, Edelman R, Nardin E, Nussenzweig V. Quantitative *Plasmodium* sporozoite neutralization assay (TSNA). J Immunol Methods 2004;292(September (1–2)):157–64.
[15] Kaslow DC. Transmission blocking vaccines. In: Hoffman SL, editor. Malaria vaccine development. Washington, DC: ASM Press; 1996. p. 181–228.
[16] Hisaeda H, Collins WE, Saul A, Stowers AW. Antibodies to *Plasmodium vivax* transmission-blocking vaccine candidate antigens Pv25 and Pvs28 do not show synergism. Vaccine 2001;20(5–6):763–70.
[17] Peiris JS, Premawansa S, Ranawaka MB, Udagama PV, Munasinghe YD, Nanayakkara MV, et al. Monoclonal and polyclonal antibodies both block and enhance transmission of human *Plasmodium vivax* malaria. Am J Trop Med Hyg 1988;39(July (1)):26–32.
[18] Carter R. Transmission blocking malaria vaccines. Vaccine 2001;19(March (17–19)):2309–14.
[19] Malkin EM, Durbin AP, Diemert DJ, Sattabongkot J, Wu Y, Miura K, et al. Phase I clinical trial of Pvs25H: a transmission blocking vaccine for *Plasmodium vivax* malaria. Vaccine 2005;23:3131–8.
[20] Stowers A, Carter R. Current developments in malaria transmission-blocking vaccines. Expert Opin Biol Ther 2001;1:619–28.
[21] Arakawa T, Tsuboi T, Kishimoto A, Sattabongkot J, Suwanabun N, Rungruang T, et al. Serum antibodies induced by intranasal immunization of mice with *Plasmodium vivax* Pvs25 co-administered with cholera toxin completely block parasite transmission to mosquitoes. Vaccine 2003;21(July (23)):3143–8.
[22] Hagiwara Y, Iwasaki T, Asanuma H, Sato Y, Sata T, Aizawa C, et al. Effects of intranasal administration of cholera toxin (or Escherichia coli heat-labile enterotoxin) B subunits supplemented with a trace amount of the holotoxin on the brain. Vaccine 2001;19(February (13–14)):1652–60.
[23] Tirawanchai N, Winger LA, Nicholas J, Sinden RE. Analysis of immunity induced by the affinity-purified 21-kilodalton zygote-ookinete surface antigen of *Plasmodium berghei*. Infect Immun 1991;59(January (1)):36–44.
[24] Sinden RE. Molecular interactions between Plasmodium and its insect vectors. Cell Microbiol 2002;4:713–24.
[25] Aregawi M, Cibulskis R, Otten M, Williams R, Dye C. World Health Organisation, World Malaria Report; 2008.
[26] Wu Y, Ellis RD, Shaffer D, Fontes E, Malkin EM, Mahanty S, et al. Phase 1 trial of malaria transmission blocking vaccine candidates Pfs25 and Pvs25 formulated with montanide ISA 51. PLoS ONE 2008;3(7):e2636.
[27] Tsuboi T, Takeo S, Iriko H, Jin L, Tsuchimochi M, Matsuda S, et al. Wheat germ cell-free system-based production of malaria proteins for discovery of novel vaccine candidates. Infect Immun 2008;76(April (4)):1702–8.
[28] Yoshida S, Araki H, Yokomine T. Baculovirus-based nasal drop vaccine confers complete protection against malaria by natural boosting of vaccine-induced antibodies in mice. Infect Immun 2010;78(February (2)):595–602.
[29] Hisaeda H, Collins WE, Saul A, Stowers AW. Antibodies to *Plasmodium vivax* transmission-blocking vaccine candidate antigens Pvs25 and Pvs28 do not show synergism. Vaccine 2001;20(December (5–6)):763–70.
[30] Abe T, Hemmi H, Miyamoto K, Morhhshi S, Tamura H, Takaku S, et al. Involvement of the Toll-like receptor 9 signalling pathway in the induction of innate immunity by baculovirus. J Virol 2005;79:2847–58.
[31] Kaslow DC, Bathurst IC, Barr PJ. Malaria transmission-blocking vaccines. Trends Biotechnol 1992;10(11):388–91.
[32] Vermeulen AN, Ponnudurai T, Beckers PJ, Verhave JP, Smits MA, Meuwissen JH. Sequential expression of antigens on sexual stages of *Plasmodium falciparum* accessible to transmission-blocking antibodies in the mosquito. J Exp Med 1985;162(5):1460–76.
[33] LeBlanc R, Vasquez Y, Hannaman D, Kumar N. Markedly enhanced immunogenicity of a Pfs25 DNA-based malaria transmission-blocking vaccine by in vivo electroporation. Vaccine 2008;26(January (2)):185–92.
[34] Lobo CA, Dhar R, Kumar N. Immunization of mice with DNA-based Pfs25 elicits potent malaria transmission-blocking antibodies. Infect Immun 1999;67(April (4)):1688–93.

THE JOURNAL OF BIOLOGICAL CHEMISTRY VOL. 285, NO. 35, pp. 26889–26899, August 27, 2010

Two Atypical L-Cysteine-regulated NADPH-dependent Oxidoreductases Involved in Redox Maintenance, L-Cystine and Iron Reduction, and Metronidazole Activation in the Enteric Protozoan *Entamoeba histolytica*[*] [S]

Received for publication, January 24, 2010, and in revised form, June 28, 2010 Published, JBC Papers in Press, June 30, 2010, DOI 10.1074/jbc.M110.106310

Ghulam Jeelani[‡§1], **Afzal Husain**[‡], **Dan Sato**[¶], **Vahab Ali**[‖], **Makoto Suematsu**[**], **Tomoyoshi Soga**[¶], **and Tomoyoshi Nozaki**[‡1,2]

From the [‡]*Department of Parasitology, National Institute of Infectious Diseases, 1-23-1 Toyama, Shinjuku-ku, Tokyo 162-8640, Japan, the* [§]*Center for Integrated Medical Research, School of Medicine, Keio University, Shinjuku, Tokyo 160-8582, Japan, the* [¶]*Institute for Advanced Biosciences, Keio University, Tsuruoka, Yamagata 997-0052, Japan, the* [‖]*Department of Biochemistry, Rajendra Memorial Research Institute of Medical Sciences, Agamkuan, Patna-800007, India, and the* [**]*Department of Biochemistry and Integrative Medical Biology, School of Medicine, Keio University, Shinjuku, Tokyo 160-8582, Japan*

We discovered novel catalytic activities of two atypical NADPH-dependent oxidoreductases (EhNO1/2) from the enteric protozoan parasite *Entamoeba histolytica*. EhNO1/2 were previously annotated as the small subunit of glutamate synthase (glutamine:2-oxoglutarate amidotransferase) based on similarity to authentic bacterial homologs. As *E. histolytica* lacks the large subunit of glutamate synthase, EhNO1/2 were presumed to play an unknown role other than glutamine/glutamate conversion. Transcriptomic and quantitative reverse PCR analyses revealed that supplementation or deprivation of extracellular L-cysteine caused dramatic up- or down-regulation, respectively, of EhNO2, but not EhNO1 expression. Biochemical analysis showed that these FAD- and 2[4Fe-4S]-containing enzymes do not act as glutamate synthases, a conclusion which was supported by phylogenetic analyses. Rather, they catalyze the NADPH-dependent reduction of oxygen to hydrogen peroxide and L-cystine to L-cysteine and also function as ferric and ferredoxin-NADP$^+$ reductases. EhNO1/2 showed notable differences in substrate specificity and catalytic efficiency; EhNO1 had lower K_m and higher k_{cat}/K_m values for ferric ion and ferredoxin than EhNO2, whereas EhNO2 preferred L-cystine as a substrate. In accordance with these properties, only EhNO1 was observed to physically interact with intrinsic ferredoxin. Interestingly, EhNO1/2 also reduced metronidazole, and *E. histolytica* transformants overexpressing either of these proteins were more sensitive to metronidazole, suggesting that EhNO1/2 are targets of this anti-amebic drug. To date, this is the first report to demonstrate that small subunit-like proteins of glutamate synthase could play an important role in redox maintenance, L-cysteine/L-cystine homeostasis, iron reduction, and the activation of metronidazole.

Glutamate synthase (glutamine:2-oxoglutarate amidotransferase, GOGAT[3]) is an iron sulfur flavoprotein that catalyzes the transfer of the amide group of L-glutamine to 2-oxoglutrate to yield L-glutamate and is a key enzyme in the nitrogen assimilation pathway. In eubacteria, this enzyme is dependent on the pyridine nucleotide NAD(P)H for its reducing equivalents and is composed of large 150-kDa (α) and small 50-kDa (β) subunits that together form the active $\alpha\beta$ protomer (1). The structural genes encoding the α and β subunit polypeptides are commonly designated *gltB* and *gltD*, respectively, and lie adjacent on the chromosome with the α subunit preceding the β subunit, except in γ-proteobacteria, where the gene order is reversed. The small subunit of eubacterial glutamate synthase shows sequence similarity to several other protein domains and enzyme subunits (2, 3) and is, therefore, proposed to represent a prototype domain used in many different cellular processes to transfer electrons from NAD(P)H to an acceptor protein or protein domain of unknown function (4). In concord with this view, numerous organisms have been recently identified to possess glutamate synthase β subunit-like genes based on DNA sequence homology (4, 5); however, the organisms often lack a gene encoding the corresponding α subunit, or the β subunit is not present adjacent to the α subunit and is, therefore, transcribed independently (5, 6). To our knowledge, among the organisms lacking a putative GOGAT α subunit, only the GOGAT β subunit from *Thermococcus kodakaraensis* (renamed from *Pyrococcus* sp. KOD1) has been functionally associated with independent GOGAT activity (7).

* This work was supported by Grants-in-aid for Scientific Research 18GS0314, 18050006, and 18073001 (to T. N.) from the Ministry of Education, Culture, Sports, Science, and Technology of Japan, a grant for research on emerging and re-emerging infectious diseases from the Ministry of Health, Labour, and Welfare of Japan (H20-Shinkosaiko-016), and a grant for research to promote the development of anti-AIDS pharmaceuticals from the Japan Health Sciences Foundation (to T. N.).

[S] The on-line version of this article (available at http://www.jbc.org) contains supplemental Figs. S1–S3.

The nucleotide sequence(s) reported in this paper has been submitted to the GenBank™/EBI Data Bank with accession number(s) AB521132 and AB521133.

[1] Supported in part by the Global Center of Excellence Program for Human Metabolomic System Biology of the Ministry of Education Culture, Sports, Science, and Technology.

[2] To whom correspondence should be addressed. Tel.: 81-3-5285-1111 (ext. 2600); Fax.: 81-3-5285-1219; E-mail: nozaki@nih.go.jp.

[3] The abbreviations used are: GOGAT, glutamine:2-oxoglutarate amidotransferase; EhNO, *E. histolytica* NADPH-dependent oxidoreductase; rEhNO, recombinant EhNO; INT, iodonitrotetrazolium; CE, capillary electrophoresis; SoFd, *S. oleracea* ferredoxin; EhFd1, *E. histolytica* ferredoxin.

Entamoeba histolytica, the causative agent of human amebiasis, is an enteric protozoan parasite responsible for amebic colitis and extraintestinal abscesses in approximately 50 million inhabitants of endemic areas (8). As is the case with other microaerophilic parasitic infections, such as giardiasis and trichomoniasis, the 5-nitroimidazole drug metronidazole has been established as the most effective treatment of amebiasis. Because of the high prevalence of these infections (9) and because of its role as a second-line defense against *Helicobacter pylori* infections (10), metronidazole has been included in the list of "essential medicines" by the World Health Organization (11). Metronidazole is a prodrug that requires reduction of the nitro group to generate the cytotoxic nitroradical anion that undergoes further reduction resulting in the generation of nitrosoimidazole (12, 13). This active form can then react with sulfhydryl groups (14) and DNA (15) while being further reduced to an amine via a hydroxylamine intermediate. Here, we report for the first time multiple novel roles of two GOGAT β subunit-like proteins in *E. histolytica*. We demonstrated that they are not associated with glutamate synthase activity but instead exhibit robust reductase activities against L-cystine, ferredoxin, and ferric ion and are also involved in the response to oxidative stress. In addition, we showed that these enzymes can be capable of reducing and activating metronidazole and, thus, are responsible for its observed toxicity against *E. histolytica*. We designated the novel NADPH-dependent oxidoreductases as EhNO1 and -2.

EXPERIMENTAL PROCEDURES

Chemicals and Reagents—L-Cysteine, L-cystine, *trans*-epoxysuccinyl-L-leucylamido-(4-guanidino) butane, cytochrome *c*, iodonitrotetrazolium (INT), and metronidazole were purchased from Sigma. Nickel-nitrilotriacetic acid-agarose was purchased from Merck. All other chemicals of analytical grade were purchased from Wako Pure Chemical (Osaka, Japan) unless otherwise stated.

Microorganisms and Cultivation—Trophozoites of the *E. histolytica* clonal strain HM1:IMSS cl 6 were maintained axenically in Diamond's BI-S-33 medium at 35.5 °C as described previously (16, 17). Trophozoites were harvested in the late logarithmic growth phase for 2–3 days after inoculation of 1/30 to 1/12 of the total culture volume. After the cultures were chilled on ice for 5 min, trophozoites were collected by centrifugation at 500 × *g* for 10 min at 4 °C and washed twice with ice-cold PBS (pH 7.4). *Escherichia coli* BL21 (DE3) strain was purchased from Invitrogen.

Quantitative Real-time PCR—Trophozoites were cultured in BI-S-33 medium supplemented with or without 10 mM L-cysteine (18 or 8 mM final, respectively). After placing the culture on ice for 5 min, the trophozoites were harvested by centrifugation at 500 × *g* for 5 min at 4 °C. Polyadenylated RNA was extracted from ~6×10^6 tropozoites with an mRNA isolation kit (Stratagene, La Jolla, CA) and then treated with deoxyribonuclease I (Invitrogen). cDNA was reverse-transcribed with 4 μg of isolated polyadenylated RNA, the SuperScript III First-Strand Synthesis System, and an oligo$(dT)_{20}$ primer (Invitrogen). PCR was performed with the resulting cDNA as a template and specific oligonucleotide primers using the ABI PRISM 7300 Sequence Detection System (Applied Biosystems, Japan). The primers used were 5′-AGCTGCACCAGTTCCAATTC-3′ and 5′-CAATCCCCAGCTGCATATAA-3′ (EhNO1), 5′-CAGTTCCAATTCCAGGCAGT-3′ and 5′-TTGGTCCTGTAACACAATCTCCT-3′ (EhNO2), and 5′-GATCCAACATATCCTAAAACAACA-3′ and 5′-TCAATTATTTTCTGACCCGTCTTC-3′ (RNA polymerase II 15-kDa subunit, GenBank™ accession number XM_643999). The parameters for PCR were as follows: an initial step of denaturation at 95 °C for 9 min followed by 40 cycles of denaturation at 94 °C for 30 s, annealing at 50 °C for 30 s, and extension at 65 °C for 1 min and a final step at 95 °C for 9 s, 60 °C for 9 s, and 95 °C for 9 s was used to remove primer dimers.

Amino Acid Comparison and Phylogenetic Analysis—Amino acid sequences of the GOGAT β subunit and β subunit-like proteins from 40 other organisms were obtained from the DDBJ/EBI/GenBank™ data base using BLASTP searches with the novel amebic NADPH-dependent oxidoreductases (EhNO1 and EhNO2) described in this paper as queries. Sequence alignments of these proteins were generated using the ClustalW program (18). The alignments obtained by ClustalW were inspected and manually corrected using the Genedoc program (19). After the removal of all gaps, 326 unambiguously aligned residues were selected for phylogenetic analyses. The neighbor-joining and maximum parsimony methods were used to construct a final phylogenetic tree for 32 sequences using the MEGA4.1 program (20). The branch lengths and bootstrap values of 1000 replicates (in percentage) in these trees were obtained from the neighbor-joining analysis.

Construction of Plasmids—Standard techniques were used for cloning and plasmid construction, as previously described (21). Genes encoding EhNO1 and EhNO2 were cloned to produce a fusion protein containing a histidine tag (provided by the vector) at the amino terminus. The cDNA corresponding to the open reading frames of EhNO1 and EhNO2 was amplified by PCR using an *E. histolytica* cDNA library (22) as a template and oligonucleotide primers. The sense and antisense oligonucleotide primers used to amplify EhNO1 and EhNO2 were 5′-CTTATAA**GGATCC**ATGAAGAGTTTCAACATTA-3′ and 5′-ATA**GTCGAC**TTAATCTTGTTCCATTGGG-3′ (EhNO1) and 5′-CTTATAA**GGATCC**ATGGCTGCTAATTATAATA-3′ and 5′-ATA**GTCGAC**TTATTCTTCATTTTTTTTACCC-3′ (EhNO2) (bold letters indicate BamHI and SalI restriction sites). PCR was performed with Platinum *Pfx* DNA polymerase (Invitrogen) and the following parameters: an initial incubation at 94 °C for 2 min followed by 30 cycles of denaturation at 94 °C for 15 s, annealing at 45 °C for 30 s, and elongation at 68 °C for 2 min and a final extension at 68 °C for 10 min. The PCR fragments were digested with BamHI and SalI, subjected to gel electrophoresis, excised, purified with the Gene clean kit II (BIO 101, Vista, CA), and then ligated into BamHI- and SalI-digested pCOLD I (Takara Bio, Otsu, Japan) in the identical orientation as the T7 promoter to generate pCOLD1-EhNO1 and pCOLD1-EhNO2. The nucleotide sequences of the cloned EhNO1 and EhNO2 genes were verified by sequencing to be identical to the putative protein coding

regions of XP_656997 and XP_653573, respectively, in *E. histolytica*.

Bacterial Expression and Purification of Recombinant EhNO (rEhNO)—The pCOLD1-EhNO1 and pCOLD1-EhNO2 expression constructs were introduced into competent *E. coli* BL21 (DE3) cells by heat shock at 42 °C for 30 s, and the resulting transformants were grown at 37 °C in 100 ml of Luria Bertani medium in the presence of 50 μg/ml ampicillin. The overnight culture was then used to inoculate 500 ml of fresh medium, which was further cultured at 37 °C with shaking at 180 rpm. When the A_{600} reached 0.6, 1 mM isopropyl β-D-thiogalactopyranoside was added to induce protein expression, and cultivation was continued for 24 h at 15 °C. The *E. coli* cells were then harvested by centrifugation at 4050 × *g* for 20 min at 4 °C, and the resulting cell pellet was washed with PBS (pH 7.4) and re-suspended in 20 ml of lysis buffer (50 mM Tris-HCl (pH 8.0), 300 mM NaCl, and 10 mM imidazole) containing 0.1% Triton X-100 (v/v), 100 μg/ml lysozyme, and 1 mM phenylmethylsulfonyl fluoride. After a 30-min incubation at room temperature, the cells were sonicated on ice and centrifuged at 25,000 × *g* for 15 min at 4 °C. The supernatant was mixed with 1.2 ml of a 50% nickel-nitrilotriacetic acid His-bind slurry (Qiagen, Tokyo, Japan) and incubated for 1 h at 4 °C with gentle shaking. The rEhNO-bound resin was washed three times with buffer A (50 mM Tris-HCl (pH 8.0), 300 mM NaCl, and 0.1% Triton X-100, v/v) containing 10–50 mM imidazole, and bound proteins were then eluted with buffer A containing 100–300 mM imidazole. After the integrity and purity of the rEhNO proteins were confirmed by 12% SDS-PAGE analysis and Coomassie Brilliant Blue staining, they were extensively dialyzed twice against a 300-fold volume of 50 mM Tris-HCl, 150 mM NaCl, pH 8.0, containing 10% glycerol (v/v) and the Complete Mini Protease Inhibitor Mixture (Roche Applied Science) for 18 h at 4 °C. The concentrations of the dialyzed proteins were spectrophotometrically determined by the Bradford method using bovine serum albumin as a standard as previously described (23). The rEhNO proteins were stored at −80 °C in 20% glycerol in small aliquots until needed.

Analysis of Prosthetic Groups—UV-visible absorption spectra of rEhNO1 (400 μg) and rEhNO2 (200 μg) were measured under both non-reducing and sodium dithionite-reducing conditions. The purified recombinant proteins were reduced with a 10-fold molar excess of sodium dithionite in 200 μl. Flavin was liberated from the recombinant enzymes by boiling samples for 10 min and then separated from proteins by centrifugation at 14,000 × *g* for 10 min. To determine whether FAD or FMN formed a prosthetic group, the fluorescence with excitation and emission wavelengths of 450 and 535 nm, respectively, was measured at pH 2.6 and 7.7 according to the method of Faeder and Siegel (24) using a fluorescence spectrophotometer (model F-2500; Hitachi).

Iron Assay—The iron content of EhNOs was determined by the *O*-phenanthroline method as previously described (25). Briefly, 60 μl samples of rEhNO1 and rEhNO2 were mixed with 4 μl of concentrated HCl and then diluted with distilled water to 0.2 ml. After the resulting mixtures were heated to 80 °C for 10 min and cooled to room temperature, they were then mixed with 0.6 ml of water, 40 μl of 10% hydroxylamine hydrochloride, and 0.2 ml of 0.1% *O*-phenanthroline and further incubated at room temperature for 30 min. The absorbances at 512 nm (A_{512}) were then measured, and the iron concentrations were determined by comparison to a standard curve generated with 0–100 μM ferrous sulfate.

Enzyme Assays—Glutamate synthase activity was assayed spectrophotometrically by measuring the rate of NADPH or NADH oxidation at 340 nm with slight modifications of the procedure described by Jongsareejit *et al.* (7). The 200-μl assay mixture contained 20 mM potassium phosphate buffer, pH 7.5, 5 mM concentrations each of L-glutamine and 2-oxoglutarate, 0.4 mM cofactor (NADPH or NADH), and varying concentrations of rEhNO proteins. The reaction was initiated by the addition of cofactor and was performed at 37 °C. To test for ammonia-dependent activity, glutamine was replaced with 100 mM NH_4Cl.

Oxidoreductase Activity—The NADPH-dependent reduction of menadione was monitored in a coupling assay under aerobic conditions. The rate of reduction of cytochrome *c* by menadione was monitored by the absorbance at 550 nm (ϵ_{550} = 21.1 mM^{-1} cm^{-1}). Measurements were made in 50 mM Tris-HCl (pH 7.5), 200 μM NADPH, 1 μM menadione, and 30 μM cytochrome *c*. The reactions were initiated by the addition of 2 μg of rEhNO1/2.

For the other electron acceptors tested, a standard mixture containing 0.1 mM NADPH, 50 mM Tris-HCl (pH 7.5), and either 0.5 mM INT, 1 mM potassium ferricyanide, or 10 mM paraquat was used. The reactions were initiated by the addition of 2 μg of rEhNO1/2 enzyme, and the reduction of the acceptors was monitored spectrophotometrically at 490 nm for INT (ϵ = 18.5 mM^{-1} cm^{-1}), 410 nm for potassium ferricyanide (ϵ = 1 mM^{-1} cm^{-1}), and 340 nm for paraquat (NADPH oxidation, ϵ = 6.22 mM^{-1} cm^{-1}). One unit of enzyme activity was defined as the formation of 1 μmol of product/min/mg of protein.

Metronidazole reduction activity was determined by measuring the oxidation of NADPH at 340 nm (ϵ_{340} = 6.22 mM^{-1} cm^{-1}) or the reduction of metronidazole at 360 nm (ϵ_{360} = 9.2 mM^{-1} cm^{-1}), as described by Chen and Blanchard (26). Assays were conducted at room temperature under strict anaerobic conditions. The reactions were initiated by the addition of 2 μg of rEhNO protein to a mixture comprising 50 mM Tris-HCl (pH 8.0), 0.5 mM metronidazole, and 0.2 mM NADPH.

The cystine reductase activity was calculated as μmol of NADPH oxidized per min at 340 nm. The assay mixture contained 0.1 M potassium phosphate (pH 7.5), 2 mM EDTA, 0.05–0.2 mM NADPH, and 0.1–5 mM L-cystine. Approximately 2 μg of rEhNO1/2 was added to initiate the reaction, and the change in absorbance at 340 nm was monitored. The effects of sulfydryl-dependent inhibitors were examined by preincubation of 2 μg of rEhNO1 and rEhNO2 with 0.1–5 mM *N*-ethylmaleimide for 10 min before the various assays. All sample reactions were performed in triplicate at a minimum.

NAD(P)H:flavin oxidoreductase activity was assayed by measuring the initial rate of NAD(P)H oxidation at 340 nm (ϵ = 6.22 $mM^{-1}cm^{-1}$) at 25 °C as described by Lo and Reeves (27). One unit of NAD(P)H:flavin oxidoreductase activity was defined as the amount of enzyme that catalyzed the oxidation of 1 μmol of NAD(P)H/min.

Ferric reductase activity was determined by measuring the difference of NAD(P)H consumption at 340 nm in the presence and absence of Fe(III) ammonium citrate. Reaction mixtures containing 0.2 mM NADPH, 100 mM Tris-HCl (pH 7.5), 0.005–1 mM ferric ammonium citrate, and 2 μg of rEhNO1 and -2 were used for the assays.

Ferredoxin-$NADP^+$ reductase activity was determined by measuring ferredoxin-dependent reduction of cytochrome *c* (28). Activity was measured by monitoring cytochrome *c* reduction at 550 nm ($\epsilon = 21.1\ mM^{-1}\ cm^{-1}$) in a reaction mixture containing 0.1 mM NADPH, 0.01–0.5 μM ferredoxin, 10 μM cytochrome *c*, and 50 mM Tris-HCl buffer (pH 7.5). The reactions were initiated by the addition of 1 μg of rEhNO1 and -2.

Determination of H_2O_2 Formation—The ferrithiocyanate method (29) was used to measure H_2O_2 formation at various time points (1–30 min) during the NADPH:favin oxidoreductase reaction. After the reactions were terminated by the addition of 0.125 volumes of 50% trichloroacetic acid, the samples were centrifuged at 12,000 × *g*, and 0.2 volumes of 10 mM ferrous ammonium sulfate and 0.1 volumes of 2.5 M potassium thiocyanate were then added. In the presence of H_2O_2, Fe^{2+} is oxidized, resulting in a colored thiocyanate-Fe^{3+} complex that can be measured by its absorption at 480 nm. The quantity of H_2O_2 formed was determined by comparison of the A_{480} values to standard curves generated using known amounts of H_2O_2.

Metabolite Extraction—Approximately 1.5 × 10^6 *E. histolytica* cells were harvested after 48 h of cultivation and washed twice with 5% mannitol. The cells were then resuspended in 1.6 ml of methanol containing 20 μM concentrations of the internal standard methionine sulfone acid and mixed with 1.6 ml of chloroform and 640 μl of deionized water. After vortexing, the mixture was centrifuged at 4600 × *g* at 4 °C for 5 min, and the aqueous layer (1.6 ml) was filtrated using an Amicon Ultrafree-MC ultrafilter (Corporation, Billerica, MA) by centrifugation at 9100 × *g* at 4 °C for ~2 h. The filtrate was dried and preserved at −80 °C until mass spectrometric analysis.

Instrumentation and Capillary Electrophoresis (CE)-Time of Flight Mass Spectrometry (TOFMS) Conditions—CE-TOFMS was carried out using an Agilent CE Capillary Electrophoresis System equipped with an Agilent 6210 Time-of-Flight mass spectrometer, Agilent 1100 isocratic HPLC pump, Agilent G1603A CE-MS adapter kit, and Agilent G1607A CE-ESI-MS sprayer kit (Agilent Technologies, Waldbronn, Germany). The system was controlled by Agilent G2201AA ChemStation software for CE. Data acquisition was performed by Analyst QS Build: 7222 software for Agilent TOF (Applied Biosystems/MDS Sciex, Ontario, Canada). Instrumental conditions for the separation and detection of metabolites were as follows. The metabolites were separated on a fused silica capillary (50 μm × 100 cm) using 1 M formic acid as the electrolyte, and the applied voltage was set at +30 kV. A solution of 50% (v/v) methanol-water was delivered as the sheath liquid at 10 μl/min (30, 31). Electrospray ionization-TOFMS was conducted in the positive ion mode (4000 V). The pressure of dry nitrogen gas was maintained at 10 p.s.i. Exact mass data were acquired over a 50–1000 *m/z* range (32, 33). Before analysis, the sample was dissolved in 20 μl of deionized water containing 200 μM concentrations of the internal standard 3-aminopyrrolidine.

Generation of E. histolytica Transformants Overexpressing EhNO—The protein coding regions of EhNO1 and EhNO2 were amplified by PCR from cDNA using sense and antisense oligonucleotides containing appropriate restriction sites at the 5′ end. The sense and antisense oligonucleotide primers used for EhNO1 and EhNO2 were 5′-CTA**CCCGGG**ATGAAGAG-TTTCAACATTACA-3′ and 5′-CAA**CTCGAG**TTAATCTT-GTTCCATTGGGGT-3′ (EhNO1) and 5′-CTA**CCCGGG**AT-GGCTGCTAATTATAATAGA-3′ and 5′-CAA**CTCGAG**TT-ATTCATTTTTTTTACC-3′ (EhNO2) (bold letters indicate restriction sites). The PCR-amplified DNA fragments were digested with SmaI and XhoI and ligated into SmaI and XhoI sites of the expression vector pKT-MR (34) to produce pKT-MR-NO1 and pKT-MR-NO2. Wild-type trophozoites were transformed with pKT-MR by liposome-mediated transfection as previously described (35). Transformants were initially selected in the presence of 3 μg/ml Geneticin (Invitrogen), which was then gradually increased to 6–20 μg/ml during the subsequent 2 weeks before subjecting the transformants to analyses.

Assay for Metronidazole Sensitivity of E. histolytica Trophozoites—To determine sensitivity to metronidazole, *E. histolytica* transfectants harboring pKT-MR-NO1, pKT-MR-NO2, or pKT-MR (control) were cultured at 37 °C in BI-S-33 medium containing 20 μg/ml Geneticin. For the assay, varying concentrations (0–16 μM) of metronidazole were added to samples containing an initial density of 10^4 cells/ml. After 48 h, the number of viable cells was counted on a hemocytometer using trypan blue to identify dead cells. The assays were performed five times in duplicate.

In Vitro Interaction of EhNO1/2 with Ferredoxin—Protein cross-linking was performed as described previously (36). Briefly, EhNO1/2 and ferredoxin (4 and 20 μM, respectively) were cross-linked by treatment with 5 mM *N*-ethyl-3-(3-dimethylaminopropyl)carbodiimide in 25 mM sodium phosphate, pH 7.5. The resulting complexes were analyzed by SDS-PAGE and Western blotting using anti-His antibody.

Immunoblot Analysis—Cell lysates and culture supernatants were separated on 12% (w/v) SDS-PAGE gels and subsequently electro-transferred onto nitrocellulose membranes (Hybond-C Extra; Amersham Biosciences) as previously described (37). Nonspecific binding was blocked by incubating the membranes for 1.5 h at room temperature in 5% nonfat dried milk in TBST (50 mM Tris-HCl (pH 8.0), 150 mM NaCl, and 0.05% Tween 20). The blots were then reacted with primary antibodies specific for EhNO1 and EhNO2 and mannose 6-phosphate receptor 1 (38) and cysteine synthase 1 (22) as controls for the membrane and cytosolic fractions, respectively, at dilutions of 1:500 to 1:100. Antisera against purified rEhNO1 and rEhNO2 were raised in rabbits commercially (Operon, Tokyo, Japan). The membranes were washed with TBST and further reacted with horseradish peroxidase-conjugated anti-rabbit or anti-mouse IgG antisera (1:20,000) (Invitrogen) at room temperature for 1.5 h. After further washing with TBST, specific proteins were visualized and measured with a chemiluminescence detection

system (Millipore) using Scion Image software (Scion Corp., Frederick, MD) (39).

RESULTS

Identification of a GOGAT Small β Subunit Gene in E. histolytica upon L-Cysteine Supplementation—Upon analysis of the transcriptome of *E. histolytica* trophozoites cultured in medium supplemented with L-cysteine, a highly up-regulated gene (XM_648481) was previously identified.[4] Although the entire transcriptome data is described elsewhere, we attempted to characterize this gene in detail in the present study. The identified gene and a gene (XM_651905) that appeared to be very closely related in the *E. histolytica* genome data base (40) were predicted to encode proteins showing high similarity to the small β subunit of GOGAT from bacteria. The genes were designated as *E. histolytica* NADPH-dependent oxidoreductase 1 and 2 [EhNO1 (XM_651905) and EhNO2 (XM_648481)] because although the encoded proteins lacked glutamate synthase activity, they showed robust NADPH-dependent oxidoreductase activity (described below). The EhNO1 and EhNO2 genes consisted of 1347- and 1338-bp open reading frames, respectively, which were predicted to encode proteins of 448 and 445 amino acids with predicted molecular masses of 49.3 and 49.0 kDa and isoelectric points of 6.31 and 7.02, respectively.

Features of the Deduced Protein Sequence of EhNOs—The predicted amino acid sequences of the two EhNOs shared 80% mutual identity and demonstrated 20–60% identities to the small β subunit of GOGAT from Archaea, bacteria, animals, and plants. EhNO1 had the highest amino acid identities to the GOGAT β subunit-like proteins of *Chlorobium tepidum* (green sulfur bacteria) and *Methanosarcina mazei* (Archaea) (62 and 59%, respectively), whereas EhNO2 showed 61–62% identities to the small subunit of *Pyrococcus abyssi* GOGAT and the β subunit chain of formate dehydrogenase from *Moorella thermoacetica* (Archaea). Although a multiple alignment of 32 GOGAT and GOGAT-like sequences was generated using ClustalW, the comparisons of representative sequences from *E. coli*, *Clostridium saccharobutylicum*, *Azospirillum brasilense*, and *E. histolytica* were sufficient to highlight the important similarities and differences among GOGAT proteins from these organisms and between the two EhNO isotypes (supplemental Fig. S1).

All of the functional domains characteristic of GOGAT β subunits were conserved between these β subunit-like proteins (supplemental Fig. S1). Two amino-terminal cysteine clusters, $CX_2CX_4CX_3CP$ (residues 40–53 for EhNO1 and residues 41–54 for EhNO2) and $CX_3CX_3CX_3C$ (residues 87–99, EhNO1; 88–100, EhNO2), matched the conserved cysteine-rich patterns proposed to be involved in the formation of [4Fe-4S] clusters (2). Similarly, two regions (residues 137–165 and 264–293 of EhNO1, labeled "FAD-I" and "NAD(P)H", respectively) matched the conserved sequences of an ADP binding fold for the binding of FAD and NAD(P)H. Both EhNO1 and -2 shared features in the NAD(P)H binding domain with the *A. brasilense* GOGAT β-protein (41), which has been proposed to confer

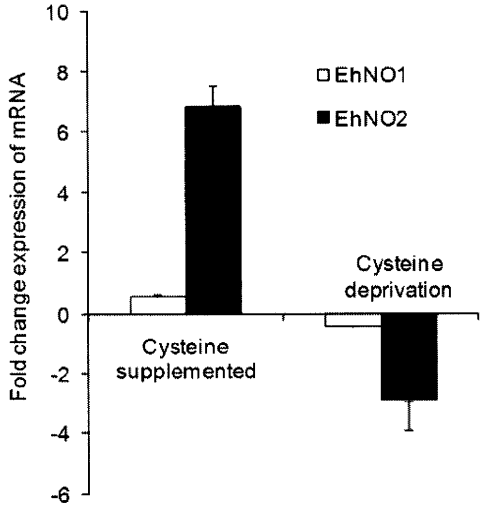

FIGURE 1. **Regulation of gene expression of EhNO isotypes in *E. histolytica* by extracellular L-cysteine concentration.** *E. histolytica* trophozoites were cultured in normal (8 mM), L-cysteine-supplemented (18 mM), or deprived medium. The expression levels of the EhNO transcripts under L-cysteine-supplemented or -deprived conditions were normalized against those of RNA polymerase II and are shown as the -fold change expression of mRNA relative to that of trophozoites from the control (normal) culture. *Error bars* represent the S.E. of three independent experiments.

specificity for NADPH, rather than NADH. The presence of alanine in place of glycine in the last residue of the motif $GXGXX$(G/A/P) (residues 269–274 of EhNO1 and 270–275 of EhNO2, shown in bold in supplemental Fig. S1) and a conserved arginine in the NAD(P)H binding domain (Arg-293 of EhNO1 and Arg-294 of EhNO2) (42) suggested that the two EhNOs prefer NADPH to NADH as a cofactor. Furthermore, a region in the carboxyl terminus (residues 401–411 of EhNO1 and 402–412 of EhNO2) matched the second FAD binding consensus sequence (TX_8GD).

Phylogenetic Analysis—Phylogenetic reconstruction was performed using neighbor-joining and maximum parsimony programs using 32 GOGAT β subunit or β subunit-like protein sequences from various organisms. The phylogenetic tree constructed using the neighbor-joining method revealed (supplemental Fig. S2) that EhNOs are more closely related to other β subunit-like homologs (supplemental Fig. S2, Group I) than to known GOGAT β subunit proteins (supplemental Fig. S2, Group II). This conclusion was also supported by the phylogenetic reconstruction using the maximum parsimony method (data not shown). Although these data did not clearly indicate the origin of the amebic GOGAT-like proteins, they suggested that EhNOs were most likely obtained by lateral gene transfer from an ancestral organism possessing a Group I-type gene, as reported previously for several other glutamate synthase β subunit-like genes (43).

Regulation of Gene Expression of EhNO Isotypes by L-Cysteine Concentration—To verify the transcriptomic data and confirm that the expression of EhNO1 and -2 was regulated by L-cysteine, the relative steady-state mRNA levels of the EhNO isotypes in *E. histolytica* trophozoites cultivated under L-cysteine-enriched or deprived conditions were measured by quantitative real-time PCR (Fig. 1). Using the RNA polymerase II 15-kDa subunit as an internal control, EhNO2 mRNA increased by

[4] A. Husain, D. Sato, G. Jeelani, M. Suematsu, T. Soga, and T. Nozaki, unpublished information.